1969

An experimental and correlative study of the equilibrium liquid and vapor phases of solutions of carbon dioxide and difluoromethane

Robert Arthur Adams
Lehigh University

AN EXPERIMENTAL AND CORRELATIVE STUDY OF THE EQUILIBRIUM LIQUID AND VAPOR PHASES OF SOLUTIONS OF CARBON DIOXIDE AND DIFLUOROMETHANE

by

Robert Arthur Adams

A Thesis

Presented in Partial Fulfillment

of the Requirements for the Degree of

Master of Science

in

Chemical Engineering

Lehigh University

1969

CERTIFICATE OF APPROVAL

This research report is accepted and approved in partial fulfillment of the requirements for the degree of Master of Science in Chemical Engineering.

June 1, 1969
(date)

Fred P. Stein
Dr. Fred P. Stein
Professor in charge

Dr. Leonard A. Wenzel
Chairman of the Department
of Chemical Engineering

DEDICATION

To my parents, whose love, devotion, and encouragement made this work possible.

ACKNOWLEDGEMENTS

I wish to express my sincere gratitude to Professor Fred P. Stein for his counsel and guidance as an advisor and, especially, as a friend.

I am indebted to the Department of Health, Education, and Welfare for its financial aid in the form of a National Defense Education Act Fellowship, and to the American Cyanamid Company for its assistance in the form of a summer grant.

The donation of the difluoromethane used in this study by the E. I. DuPont de Nemours and Company is gratefully acknowledged.

I thank Mr. Arnold Piacentini for the use of his experimental apparatus diagrams, and Mr. Joseph Hojsak for his assistance with experimental problems.

Finally, I should like to thank the graduate students of the Chemical Engineering Department, especially Messrs. David Smallwood and Patricio Proust, for their sincere interest and many helpful suggestions throughout the course of this work.

TABLE OF CONTENTS

LIST OF FIGURES

LIST OF TABLES

ABSTRACT

Experimental vapor-liquid equilibrium data for the carbon dioxide - difluoromethane binary were determined at -60, -20, 20, and 50°F. The liquid phase was observed to behave nearly ideally at each temperature level.

The data were correlated as a function of temperature and composition. The vapor phase was described by the Redlich-Kwong equation of state. The liquid-phase activity coefficients were correlated with the Redlich-Kister equation for excess free energy. The Redlich-Kister constants at each isotherm were correlated by a least-squares fit with temperature. The correlation developed predicts the vapor-liquid equilibria for this system at any temperature between -60 and 50°F.

1) INTRODUCTION AND BACKGROUND

1.1) Introduction

The selection of a refrigerant for a particular process is dictated by the physical and practical properties of the materials under consideration. Desirable physical properties include a high critical and a low freezing temperature, low liquid and vapor densities, and reasonable evaporation and condensation pressures. Practical properties of importance are cost, chemical and physical inertness, corrosiveness, toxicity, and explosiveness (1,2). Quite often this desirable range of properties for a particular application is achieved by a combination of two or more refrigerants. In particular, mixtures of fluorocarbons have undergone increased use in this respect. These compounds are for the most part nontoxic, noncorrosive, nonflammable, and physically and chemically inert.

Difluoromethane is an important exception; its flammability has restricted its development as a commercial refrigerant. In combination with a second refrigerant which is an effective fire extinguishing agent, such as

carbon dioxide, this fire hazard may be overcome. At the same time, this mixture may produce a refrigerant whose physical property range has yet to be achieved. Establishment of such a property range requires accurate thermodynamic data describing the vapor-liquid equilibria of the mixture. Accordingly, it was decided to determine experimentally the vapor-liquid equilibria of the binary system: carbon dioxide - difluoromethane (CO_2 - CH_2F_2). Carbon dioxide is a nonpolar molecule with a large quadrupole moment, while difluoromethane is highly polar.

The basic problem in the study of the thermodynamic properties of mixtures has been to relate these mixture properties to those of its components with a minimum amount of experimental information on the mixture itself. Therefore, in addition to satisfying a commercial need, this investigation is another step toward the final goal of predicting a mixture's properties using only pure-component data.

1.2) Background

While the published data on the phase equilibria of systems consisting of carbon dioxide as one of the components is abundant, those containing a fluorocarbon as a second

component are rare. Zeeninger (3) has studied the CO_2 - $CClF_3$ binary via calorimetric analysis. Studies of fluorocarbon solutions containing difluoromethane are also scarce. Scott (4,5) has reported phase diagrams and bubble-point curves at one temperature level for the binary systems: CH_2F_2 - CHF_3 and CH_2F_2 - $CClF_3$.

2) EXPERIMENTAL APPARATUS AND PROCEDURE

2.1) Introduction

An equilibrium still utilizing the vapor-recirculation technique was used throughout this work. The apparatus, built by Piacentini (6), is a modification of that designed by Stein (7). It has since been used by several other investigators for the determination of vapor-liquid equilibrium of binary fluorocarbon solutions. A flow diagram of the apparatus in Figure 1 illustrates the important features of the vapor-recirculation technique. Design specifications for the equipment have been detailed by Piacentini.

A mixture of the components is introduced into the circulation loop to establish a liquid level in the equilibrium cell. The vapor above the liquid is pumped out of the cell, passed through a vapor-sampling coil, and returned to the bottom of the cell at the temperature of the system. As the vapor bubbles up through the liquid, continuous and intimate phase contact is achieved and the attainment of equilibrium is assured.

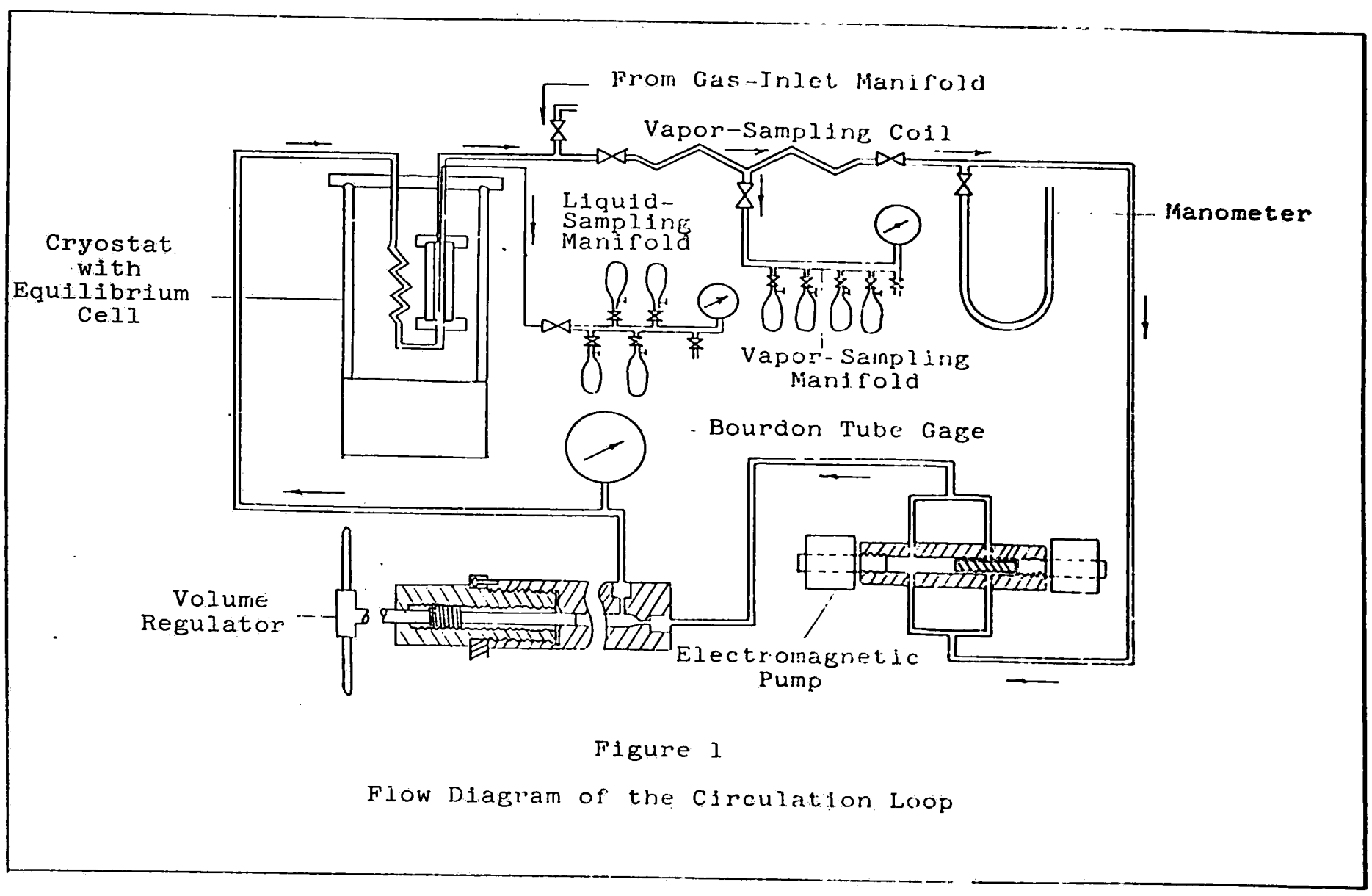

Figure 1

Flow Diagram of the Circulation Loop

2.2) Vapor-Liquid Equilibrium Cell

The equilibrium cell is suspended in the cryostat, or low-temperature bath, as illustrated in Figure 2. A coil of copper tubing, also suspended in the bath, cools the recirculating vapor from ambient air temperature to the equilibrium temperature. The cooled vapor enters the cell through five small holes which were drilled through the bottom of the stainless steel flange supporting the cell. The bubbles are dispersed through the liquid as they pass through a disc of stainless steel screen. The vapor then leaves through copper tubing at the top of the cell.

Liquid sampling is done by means of a stainless steel capillary tube which enters the cell through the vapor-outlet line. This probe leads to the liquid sampling manifold, as shown in Figure 1. The liquid level was maintained at least one-half the height of the cell to provide sufficient liquid for sampling. This minimum height also assures good vapor-liquid contact.

2.3) Vapor Circulation Loop

The vapor leaving the equilibrium cell passes through a vapor-sampling coil. This coil can be closed off to entrap a vapor sample for analysis.

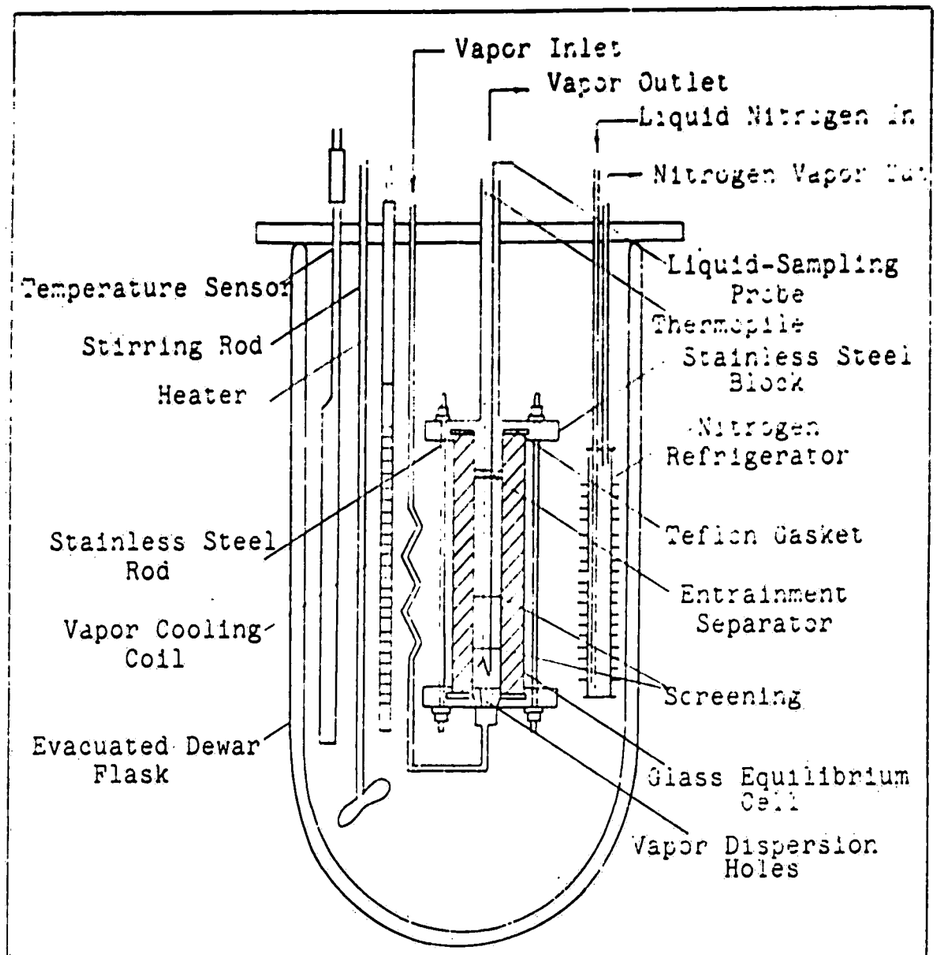

Figure 2

The Cryostat and the Equilibrium Cell

The vapor then passes through an electromagnetic pump, whose function is that of providing continuous vapor recirculation. The basic design of the pump is illustrated in Figure 3. An important feature of the pump is its double acting nature which permits the volume of the system to remain constant while equilibrium is being attained. The pump is capable of producing a pressure head of about one psi, which is sufficient to force the vapor bubbles up through the liquid in the cell.

The circulating vapor leaves the pump and passes through the volume regulator before returning to the cell. The volume regulator is simply a stainless steel piston which can be screw-driven into the free space of a cylinder. During the liquid sampling procedure, as liquid is withdrawn, the pressure of the system would tend to decrease. The function of the volume regulator is then to maintain the pressure of the system constant during liquid sampling by driving the piston into the cylinder.

2.4) Temperature Measurement and Control

The temperature of the system was determined by measuring the millivoltage output of a three junction thermopile within the equilibrium cell and a single

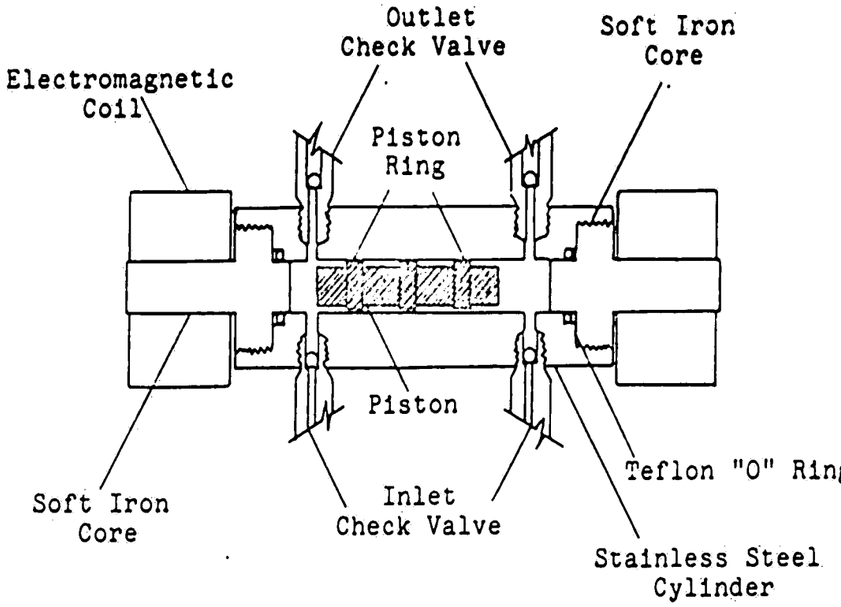

Figure 3

The Electromagnetic Circulation Pump

junction thermocouple immersed in the cryostat fluid. Measurements were taken with a Leeds and Northrup Type 3-K Universal Potentiometer using an ice bath as reference.

The thermopile and bath thermocouple were originally calibrated by Piacentini (6) and later by Smolcha (8). Tables of temperature versus millivolts were calculated by these investigators, the former doing so at temperatures of 32°F and below in 0.1°F increments, and the latter at temperatures greater than 32°F in 0.01°F increments. These calibrations were verified by measuring the vapor pressure of each of the pure components at several temperatures. The technique used and the results obtained are discussed in Sections (2.7) and (3.1), respectively.

The heat-transfer fluid used in the low-temperature bath was trichloromonofluoromethane (CCl_3F). It was contained in a clear glass Dewar flask of approximately three liters. An electric stirrer provided continuous and vigorous agitation.

The temperature was controlled with a Bayley Instrument Company precision, proportional temperature controller. The bath temperature was first cooled to

slightly below the desired equilibrium temperature by vaporizing liquid nitrogen as it passed through a copper finned heat exchanger immersed in the bath. The refrigeration supplied to the bath was then maintained at a constant rate while the bath temperature was adjusted and controlled by supplying heat at a rate determined by the controller.

2.5 Pressure Measurement

The system pressure was measured by Heise Bourdon-tube pressure gauges. As the system temperature was increased, the range of the system pressure also increased. It was therefore necessary to change pressure gauges as follows: for the -60°F isotherm, a 0-100 psia range in intervals of 0.1 psi was used; for -20 and 20°F, a 0-500 psia range in intervals of 0.5 psi; and for 50°F, a 0-1000 psia range in intervals of 1.0 psi.

2.6) Sample Analysis

2.61) Analytical Apparatus

Both the liquid and the vapor samples were analyzed using a Beckman GC-2A gas chromatograph. The composition

of each unknown phase sample was determined by comparing it with a standard sample of composition approximately that of the unknown. A charging manifold, in series with a mercury manometer and a vacuum pump, was attached to the chromatograph so that the pressure of each sample charged to the evacuated manifold could be measured. The pressure of each gas sample could be determined within an accuracy of ±0.5 mm Hg.

The chromatograph column consisted of an eighteen-foot length of one-quarter inch copper tubing packed with di-n-butyl maleate coated onto a stationary support. The chromatograph operating conditions were maintained constant throughout the study. These were as follows: carrier gas (helium) pressure, 30 psig; column temperature, 40°C; and filament current, 100 ma. The sample size varied from 220 to 600 mm Hg in a 1.0 cc sample loop. The majority of the samples were charged at 560 mm Hg.

The composition of the sample was determined by a comparison of its chromatogram peak area to that of a known standard. Each component passed through the sensing side of a thermal conductivity cell in the chromatograph. The voltage output of the cell was amplified and converted

to signals of proportional frequency by an electronic integrator. A counter mounted above the voltage-to-frequency converter then totalized these signals. The total number of counts recorded for each component was divided by the sample size to give a normalized counts per mm Hg. These normalized counts were found to be valid if the sample size varied by no more than 100 mm Hg.

2.62) Calibration Procedure

A series of nine high-pressure standard gas mixtures of known composition was prepared several weeks prior to operating the experimental apparatus. These standards were used to analyze all unknown phase samples on the gas chromatograph. The high pressure was necessary to assure sufficient standard mixture for the duration of the experimental program.

The standards were mixed in 300 cc laboratory lecture bottles at total pressures varying from 218 to 300 psia. This nonuniformity of standard size was due to the fact that the vapor pressure of the heavy component, CH_2F_2, at room temperature, was 240 psia. The maximum pressure of the mixture was therefore restricted

by the possibility of liquefaction of CH_2F_2. As a precaution, when the mole fraction of CH_2F_2 exceeded 0.25, the partial pressure of CH_2F_2, coupled with approximate corrections for nonideality, was not allowed to exceed 214 psia. For these standards, the total pressure of the mixture was not allowed to exceed 230 psia. At compositions less than 0.25 mole fraction CH_2F_2, a maximum total pressure of 300 psia was permitted, where the partial pressure of CH_2F_2 was never greater than 70 psia.

At room temperature and 300 psia, the compressibility factors of CO_2 and CH_2F_2 are 0.88 and 0.84, respectively. Attempts to determine the composition of these standards by corrections for nonideality could be grossly in error. Accordingly, a series of low-pressure primary standards was prepared, each having a composition approximately that of a high-pressure standard. The final composition of the high-pressure mixtures would then be determined by a comparison of the chromatograms of each high-pressure standard with that of a corresponding low-pressure standard of known composition.

The primary standards were prepared at a total pressure of approximately two atmospheres. Corrections

for the gas nonidealities were determined by using the pressure explicit form of the virial equation of state truncated after the second virial coefficient. This equation has the form

$$\frac{Pv}{RT} = 1 + \frac{B}{v} \qquad (2.1)$$

where v is the molar volume of the gas, and B is the second virial coefficient. For a pure component, the second virial coefficient is a function only of temperature. Second virial coefficients for each component were calculated from the Pitzer and Curl (9) correlation based on a three parameter theory of corresponding states. For the nonpolar component, CO_2, it has the following form

$$\frac{P_{ci}\, B_{ii}}{R\, T_{ci}} = f_B^{(0)}\,(T_R) + \omega_i\, f_B^{(1)}\,(T_R) \qquad (2.2)$$

where P_{ci} = critical pressure of "i"

T_{ci} = critical temperature of "i"

ω_i = acentric factor of "i"

T_R = reduced temperature, T/T_{ci}

The acentric factor is defined by

$$\omega_i \equiv - \log_{10} \left(\frac{P_i^s}{P_{ci}}\right) - 1.000 \qquad (2.3)$$

where P_i^s is the saturation (vapor) pressure of "i" at $T/T_{ci} = 0.7$.

The two empirically determined functions of reduced temperature are

$$f_B^{(0)}(T_R) = 0.1445 - \frac{0.330}{T_R} - \frac{0.1385}{T_R^2} - \frac{0.0121}{T_R^3} \qquad (2.4)$$

$$f_B^{(1)}(T_R) = 0.073 + \frac{0.46}{T_R} - \frac{0.50}{T_R^2} - \frac{0.097}{T_R^3} - \frac{0.0073}{T_R^8} \qquad (2.5)$$

Difluoromethane has a large dipole moment. Prausnitz (10) has developed an extension of the Pitzer and Curl correlation for polar gases. It has the form

$$\frac{P_{ci} B_{ii}}{R T_{ci}} = f_B^{(0)}(T_R) + \omega_{H_i} f_B^{(1)}(T_R) + f_\mu(\mu_R, T_R) + \eta_i f_a(T_R) \qquad (2.6)$$

where ω_{H_i} represents the acentric factor of the polar component's homomorph. A homomorph is a nonpolar molecule having approximately the same size and shape as those of the polar molecule. The functions $f_B^{(0)}$ and $f_B^{(1)}$ are the same as presented by Equations (2.4) and (2.5). The function $f_\mu(\mu_R, T_R)$ depends on the reduced dipole moment and the reduced temperature as follows:

$$f_\mu(\mu_R, T_R) = -5.237220 + 5.665807 \ln \mu_R - 2.133816 (\ln \mu_R)^2 + 0.2525373 (\ln \mu_R)^3 + 1/T_R [5.769770 - 6.181427 \ln \mu_R + 2.283270 (\ln \mu_R)^2 - 0.2649074 (\ln \mu_R)^3] \quad (2.7)$$

where

$$\mu_R = \frac{10^5 \mu_i^2 P_{ci}}{T_{ci}^2} \quad (2.8)$$

$$T_R = \frac{T}{T_{ci}} \quad (2.9)$$

μ_i is the dipole moment in debye, P_{ci} is the critical pressure in atmospheres, and T_{ci} is the critical temperature in degrees Kelvin. The fourth term in the correlation is a dimerization term, where η_i is the association constant. For CH_2F_2, this constant was taken to be zero.

The virial coefficients obtained by this method agreed closely with those calculated from the Martin-Hou (11,12) equation of state.

For gas mixtures, the second virial coefficients are functions of composition as well as temperature. This composition dependency is given by the following rigorous relationship

$$B_{mixture} = \sum_{i}^{N} \sum_{j}^{N} y_i y_j B_{ij} \qquad (2.10)$$

where B_{ij}, the cross-coefficient, is equal to B_{ji}. For a binary mixture

$$B_{mixture} = y_1^2 B_{11} + 2y_1y_2 B_{12} + y_2^2 B_{22} \qquad (2.11)$$

The cross-coefficient was estimated by using the following mixing rules suggested by Prausnitz (10) for the case where "i" is a nonpolar molecule and "j" is polar:

$$T_{cij} = (T_{ci}\ T_{cj})^{1/2} \tag{2.12}$$

$$\omega_{ij} = \frac{1}{2}(\omega_i + \omega_{Hj}) \tag{2.13}$$

$$P_{cij} = \frac{4\ T_{cij}\ \left[\frac{P_{ci}\ v_{ci}}{T_{ci}} + \frac{P_{cj}\ v_{cj}}{T_{cj}}\right]}{(v_{ci}^{1/3} + v_{cj}^{1/3})^3} \tag{2.14}$$

Table A-1 lists each of the low-pressure primary standards with its ideal gas composition and its final composition as corrected by the virial equation of state. It can be seen that the average deviation from ideality was 0.66 %, with maximum deviations of 2.0 to 2.9 % in the three mixtures with a high CH_2F_2 concentration. Table A-2 lists each of the high-pressure secondary standards with its final composition as determined by comparison to the corresponding primary standard.

Both the high- and low-pressure standards were prepared by means of a gas mixing apparatus equipped with

a 1000 psia Heise Bourdon-tube pressure gauge, a mercury manometer, and a McLeod vacuum gauge. The apparatus was initially evacuated to 0.05 mm Hg, purged several times with CO_2, and re-evacuated. In preparing the primary standards, the minor component was slowly introduced until the approximate desired partial pressure was attained. Five to ten minutes were allowed for temperature and pressure equilibration, at which time the partial pressure was recorded from readings taken from the mercury manometer. The major component was then introduced at a pressure greater than that of the minor component. Once again, after sufficient time for equilibration, the total pressure of the mixture was recorded. The final pressure for all primary standards was approximately 1550 mm Hg. Several days were allowed to insure adequate mixing of these standards.

The high-pressure secondary standards were prepared in the same manner as the low-pressure set, with the exception that all pressure readings were taken on the Heise gauge. Several weeks were allowed for mixing. During this time, the lecture bottles were periodically heated on one side, then allowed to cool to room temperature.

2.63) Sample Analysis Procedure

The composition of each unknown liquid and vapor sample was determined by comparing its chromatogram peak area to that of a secondary standard whose composition was as close as possible to the anticipated composition of the unknown. For samples containing the minor component in excess of ten per cent, the final compositions were determined by normalizing the values calculated for both components. Where the minor component was less than ten per cent composition, the major component was determined by difference.

2.64) Gas Impurities

The carbon dioxide purity as received was 99.8 %, and no further steps were taken to improve this purity. However, no analysis for the difluoromethane was available. Chromatographic analysis of a vapor sample of CH_2F_2 revealed the presence of an impurity in quantities of approximately one per cent. The chromatograph retention time of this impurity was nearly equal to that of the carbon dioxide, causing a distortion of the CO_2 chromatogram peak. This distortion invalidated any measurement of the CO_2 concentration.

It was suspected that the impurity was more volatile than the CH_2F_2. A portion of the gas was therefore transfered to a stainless steel cylinder, which was then submerged in a Dewar containing dry ice and acetone. The vapor space above the liquid was then evacuated for a period of several hours. The cylinder was then allowed to warm up to room temperature, and the gas was again analyzed. Although this procedure effectively reduced the impurity content to approximately 0.4 %, the CO_2 chromatogram peak remained slightly distorted. This procedure of cooling and evacuation, followed by analysis, was repeated several times with no additional improvement in purity.

However, when the cylinder was inverted and a liquid sample obtained, the chromatogram revealed the liquid contained about one-half of the impurity observed in the vapor phase. In addition, no distortion of the CO_2 peak was observed. Consequently, the cylinder was permanently mounted in an inverted position and liquid CH_2F_2 was used for all subsequent experimental work.

2.7) Experimental Procedure

The system was initially evacuated to 0.15 mm Hg, purged with CH_2F_2, and re-evacuated. The cryostat Dewar

was filled with the bath fluid and raised into position completely submerging the equilibrium cell and its surrounding devices, as illustrated in Figure 2. The electric bath stirrer was then started, and liquid nitrogen was directed into the finned-tube heat exchanger at a pressure of 6 psig. Potentiometer readings were then taken. When the temperature of the bath fell slightly below the desired operating temperature, the temperature controller was turned on. The controller set point corresponding to the equilibrium temperature was determined, and final adjustments were made by varying a rheostat connected in parallel to the control heater.

When the desired operating temperature was reached, the heavy component, CH_2F_2, was introduced until a liquid level of approximately one-half the cell height was achieved. In an extension of the purity procedure discussed in Section (2.64), the system was slightly vented in an attempt to yet improve upon the purity previously attained. The circulation pump was then started. When the system pressure reached a constant value, it was recorded as the vapor pressure of the heavy component at this operating temperature.

The light component, CO_2, was then slowly introduced into the system, taking care to prevent any drastic

changes in system pressure. The system would react to component additions first by a drop in liquid level and a rise in pressure, followed by a rise in liquid level to a level higher than that preceding the addition, and a subsequent lowering in pressure. Some minimum pressure would be reached, at which point a slight rise would again be observed. This slight rise and drop continued over a period from a few minutes to several hours, depending on the operating temperature.

At the three lower temperature levels, this fluctuation was very slight. At -60°F, this period was approximately ten minutes; at -20°F, about fifteen minutes; and at 20°F, one-half hour. It was at 50°F, however, where this phenomenon was most pronounced. At this temperature, these fluctuations continued for as long as three to four hours before pressure equilibrium was attained. At all temperature levels, once equilibrium was achieved, the gases were allowed to circulate for an additional twenty to thirty minutes at equilibrium conditions before the sampling procedure was begun.

The vapor circulation was then stopped and the system pressure was recorded. A vapor sample was trapped in the vapor-sampling manifold and directed into a

previously evacuated 75 cc high-pressure sampling cylinder. The liquid sampling consisted of first purging the liquid-sampling probe, and then directing a liquid sample through the probe and into an evacuated sampling cylinder. During the liquid sampling, the system pressure was maintained constant with the volume regulator. This sampling procedure was accomplished within thirty to sixty seconds following the shutdown of the pump.

A new operating pressure was then attained by adding CO_2 and CH_2F_2. This entire procedure was repeated until a set from five to seven different pressures had been accumulated, at which time chromatographic analysis was begun.

The number of runs which could be accomplished during one day varied from two to five, depending upon the operating temperature as discussed previously. Following the final run of the day, providing an isotherm had not been completed, the system was maintained at a pressure from 50 to 100 psig while not in operation in order to preserve internal gaseous purity. After the final run of an isotherm, the system was evacuated, and then purged with CO_2 several times. Carbon dioxide was then added to the system until a liquid level was attained

and the system pressure was then recorded as the vapor pressure at that temperature.

3) EXPERIMENTAL RESULTS AND DISCUSSION

3.1) Pure-Component Vapor Pressures

The vapor pressure of the pure components was measured at each of the four temperature levels studied. The technique for these measurements is presented in Section (2.7). These experimental data, accompanied by a comparison to published vapor pressure data, are presented in Table 1.

The carbon dioxide vapor-pressure data represent that published by the American Society of Refrigerating Engineers (13). A comparison with the experimental data shows an average deviation of 0.22 %, with a maximum deviation at -20°F of 0.33 %.

The difluoromethane vapor pressures represent those calculated at the experimental temperature levels from an equation proposed by Malbrunot (14). The equation is based on vapor pressure measurements at thirty temperature levels, none of which corresponds to those of this work. A comparison with the experimental data shows an average deviation of 0.34 %, with a maximum deviation at 20°F of 0.55 %.

Table 1

Comparison of Experimental and

Literature Vapor Pressures

Carbon Dioxide (13)

Temp., °F	Experimental Vapor Pressure, psia	Literature Vapor Pressure, psia	Per Cent Deviation
-60	94.6	94.7	0.106
-20	214.2	214.9	0.33
20	422.4	421.8	0.14
50	651.6	653.6	0.31

Difluoromethane (14)

-60	15.18	15.13	0.29
-20	41.6	41.5	0.16
20	95.2	94.7	0.55
50	161.0	160.4	0.36

3.2) Vapor-Liquid Equilibrium Data

Experimental vapor-liquid equilibrium data were determined at four temperature levels: -60, -20, 20, and 50°F. These data are tabulated in Tables B-1 to B-4, and plotted on pressure-composition diagrams in Figures 4 to 7.

Inspection of these pressure-composition diagrams reveals the liquid phase to be nearly ideal at all temperature levels studied, the ideality decreasing with the increasing temperature. At the two lower-temperature isotherms, the liquidus curves were very nearly straight lines. Using only this geometric property and the vapor-liquid equilibrium equation for each component, it can be shown that the straight liquidus line permits the vapor phase curve to be calculated from only the pure component vapor pressures. The predictive consequences of this observation are discussed in detail in Section (5.4).

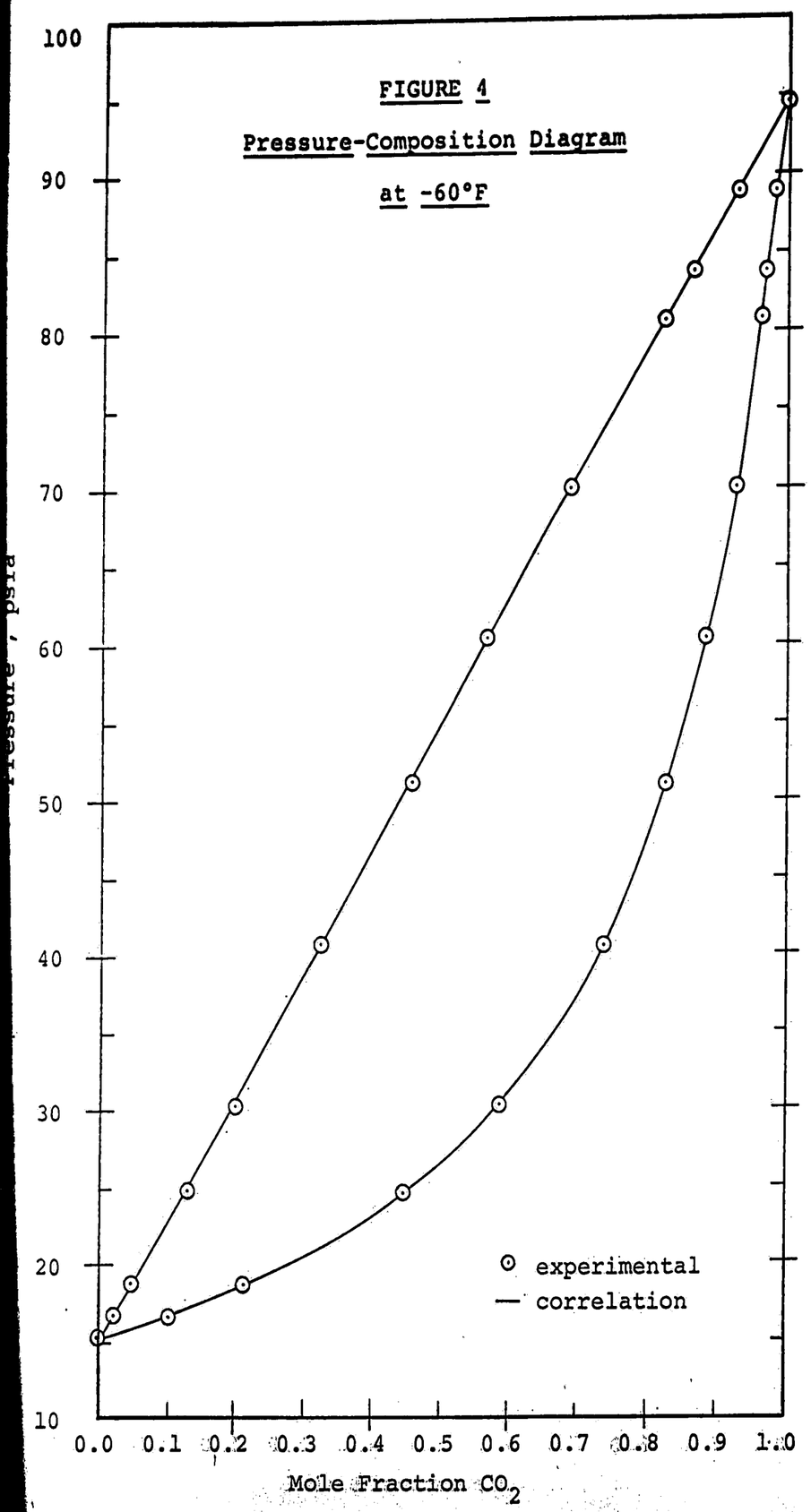
FIGURE 4
Pressure-Composition Diagram
at -60°F
Pressure, psia
100
90
80
70
60
50
40
30
20
10
0.0
0.1
0.2
0.3
0.4
0.5
0.6
0.7
0.8
0.9
1.0
Mole Fraction CO_2
experimental
correlation

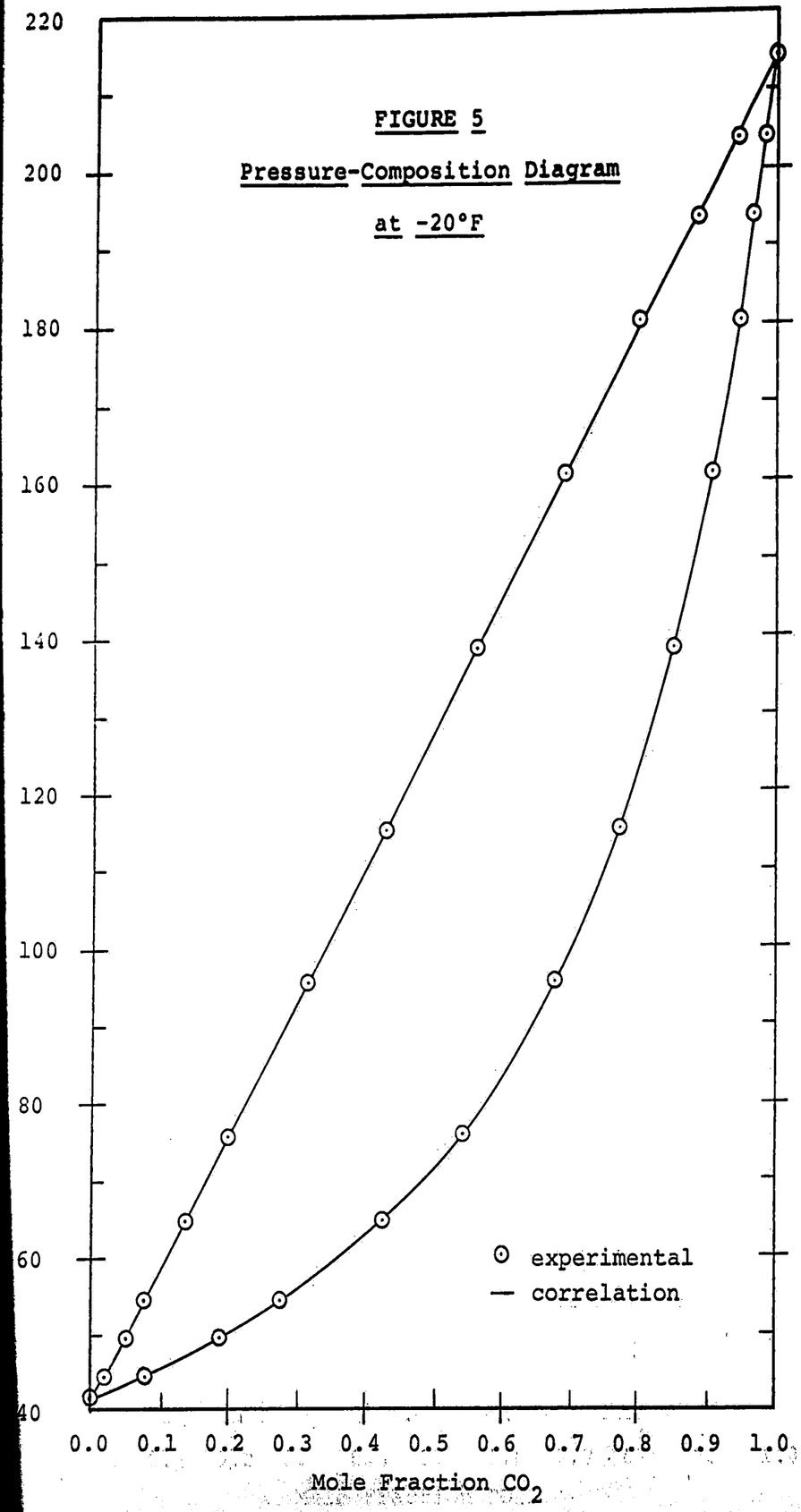

FIGURE 5

Pressure-Composition Diagram

at -20°F

FIGURE 6

Pressure-Composition Diagram

at 20°F

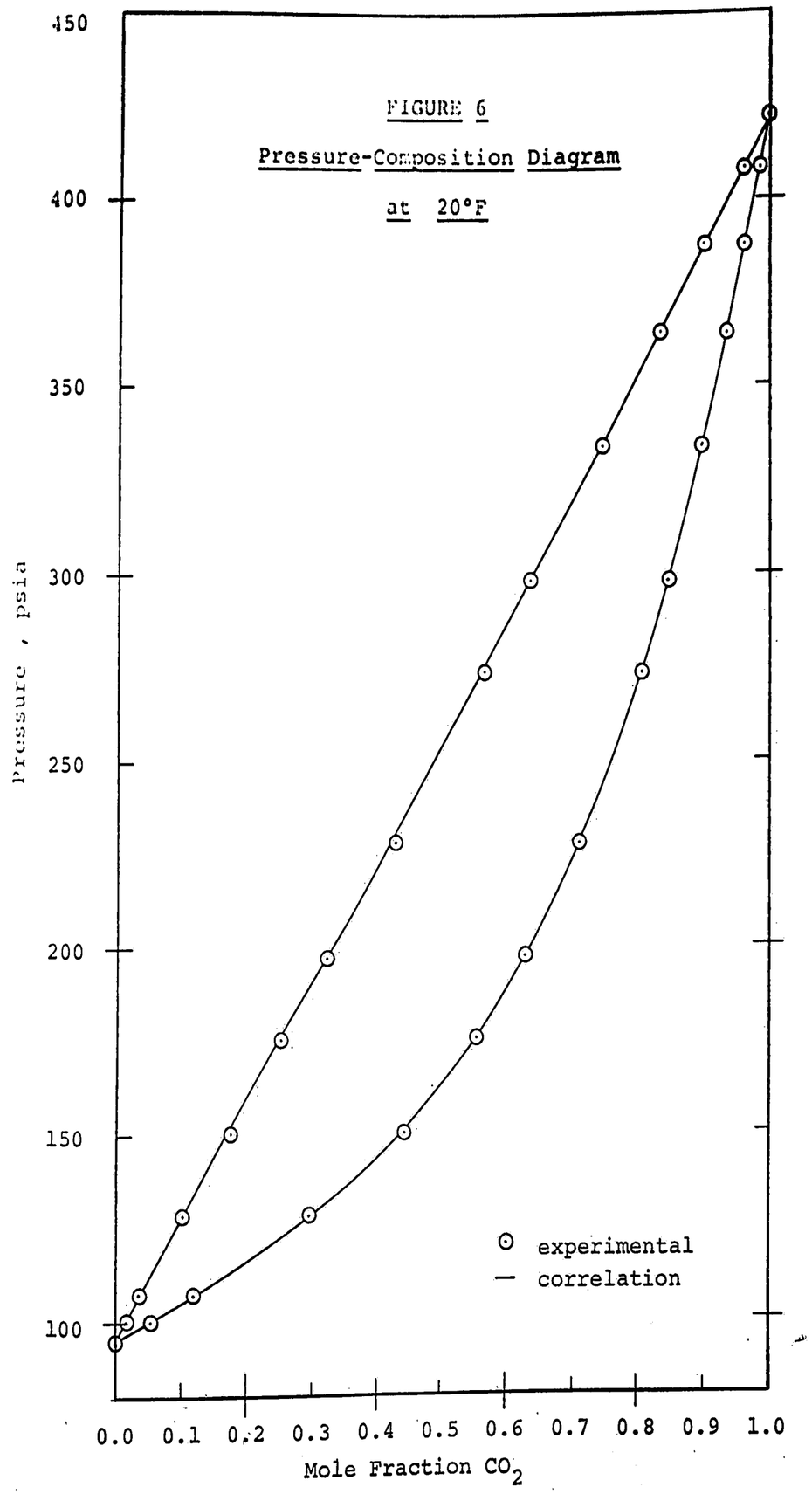

FIGURE 7

Pressure-Composition Diagram at 50°F

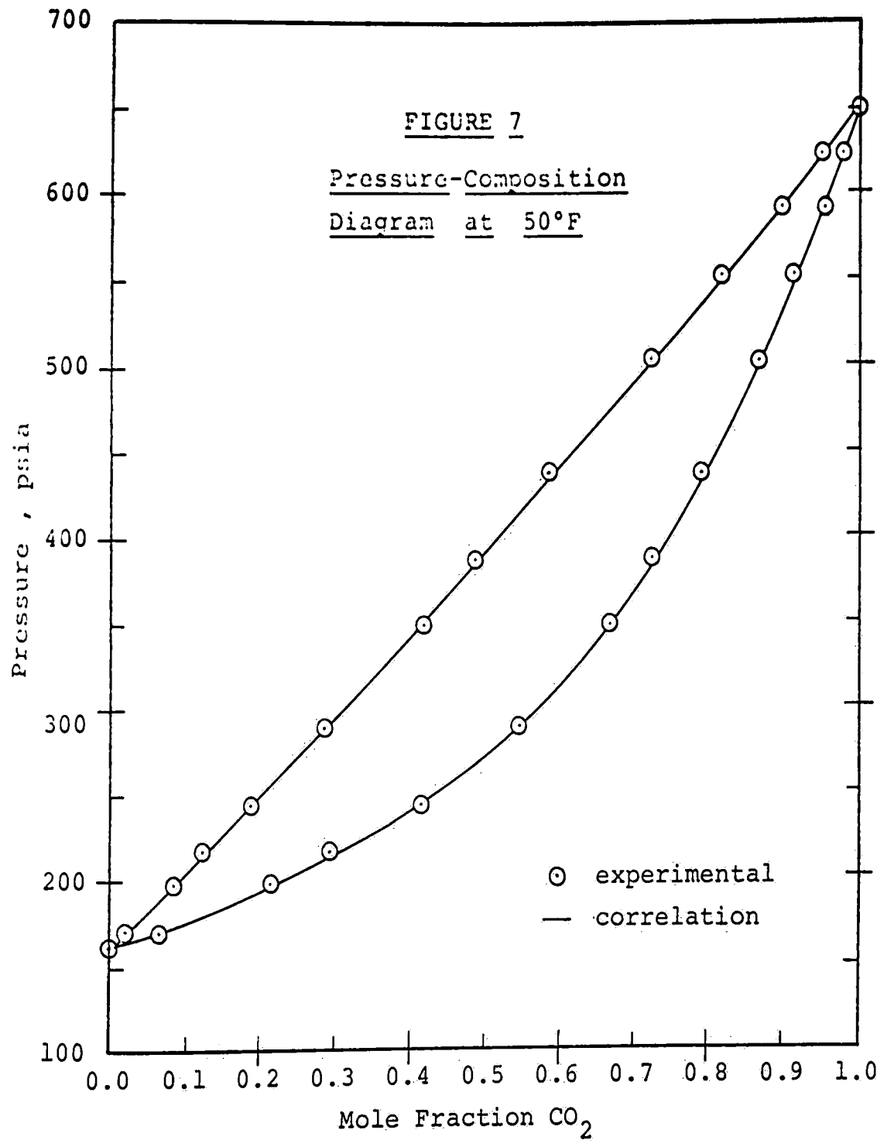

4) THERMODYNAMIC TREATMENT OF EXPERIMENTAL DATA

4.1) Introduction

The thermodynamic treatment of multicomponent phase equilibria is based on the concept of the chemical potential, or partial molal free energy, as introduced by J. Willard Gibbs (10). Thermodynamic equilibrium between a liquid phase and a vapor phase is established when the temperature of each phase is equal to that of the other and when the chemical potential of each molecular species present is the same in both phases. The concept of the chemical potential is, however, an inconvenient one mathematically, as it can be expressed only relative to some arbitrary reference state. G. N. Lewis defined a more useful quantity, the fugacity, which is directly related to the chemical potential and can be expressed in absolute values. The fugacity may be thought of as a partial pressure which is corrected for nonideal behavior in real mixtures. At low pressures, where the mixture approaches ideality, the fugacity of each component is very closely approximated by its partial pressure.

In terms of the fugacity f, the equilibrium equation for each component "i" in a liquid and a vapor phase at the same temperature becomes:

$$f_i^V = f_i^L \tag{4.1}$$

where the superscripts V and L denote the vapor and liquid phases, respectively.

This equation can be expressed in terms of the experimentally measurable quantities of temperature, pressure, and composition by defining two auxiliary functions, the fugacity coefficient and the activity coefficient.

The fugacity coefficient, ϕ_i, relates the vapor-phase fugacity of component "i", f_i^V, to its mole fraction in the vapor, y_i, and to the total system pressure, P. It is defined as follows:

$$\phi_i \equiv \frac{f_i^V}{y_i P} \tag{4.2}$$

The activity coefficient, γ_i, relates the liquid-phase fugacity of component "i", f_i^L, to its mole fraction in

the liquid, x_i, and to standard-state fugacity, f_i^{OL}. It is defined as follows:

$$\gamma_i \equiv \frac{f_i^L}{x_i f_i^{OL}} \tag{4.3}$$

The equation of equilibrium for each component "i" may be rewritten by combining equations (4.1), (4.2), and (4.3):

$$\phi_i y_i P = \gamma_i x_i f_i^{OL} \tag{4.4}$$

4.2) The Fugacity Coefficient

The fugacity coefficient is a function of temperature, total pressure, and the composition of the vapor phase. It can be evaluated from volumetric data of the vapor phase as expressed in the form of an equation of state. This equation of state is usually pressure explicit, that is, the pressure is expressed as a function of the

temperature, volume, and mole numbers.

Beattie (15) presents a rigorous thermodynamic relationship for the fugacity coefficient in terms of a pressure-explicit equation of state

$$\ln \phi_i = \frac{1}{RT} \int_V^\infty \left[\left(\frac{\partial P}{\partial n_i} \right)_{T,V,n_j} - \frac{RT}{V} \right] dV - \ln z \qquad (4.5)$$

where n_i represents the number of moles of component "i", V is the total volume of the vapor mixture, and z is the compressibility factor at temperature T and total system pressure P.

It is, therefore, necessary to specify a particular equation of state in order to obtain numerical results for the fugacity coefficient. The Redlich-Kwong equation, explicit in pressure, was used to describe the vapor phase in this work.

4.3) The Redlich-Kwong Equation of State

The Redlich-Kwong equation of state (16) has the form:

$$P = \frac{RT}{v-b} - \frac{a}{T^{0.5}\, v(v+b)} \qquad (4.6)$$

where

$$a = \frac{\Omega_a R^2 T_{ci}^{2.5}}{P_{ci}} \qquad (4.7)$$

$$b = \frac{\Omega_b RT_{ci}}{P_{ci}} \qquad (4.8)$$

If the first and second isothermal derivatives of pressure with respect to volume are set equal to zero and evaluated at the critical point, the dimensionless constants Ω_a and Ω_b are 0.4278 and 0.0867, respectively. However, in vapor-liquid equilibrium studies such as this work, interest in the volumetric behavior of saturated vapors is not focused

on the critical region only, but rather over a wide range of temperature. Prausnitz (17) proposed fitting the Redlich-Kwong equation to the volumetric data of the saturated vapor in order to evaluate Ω_a and Ω_b for each pure component studied. The range of temperature used is from the normal boiling point to the critical temperature. These parameters are listed in Table 2.

To apply the Redlich-Kwong equation to mixtures, Prausnitz proposes the following mixing rules for the constants "a" and "b":

$$b = \sum_{i=1}^{N} y_i b_i \tag{4.9}$$

where

$$b_i = \frac{\Omega_{bi} RT_{ci}}{P_{ci}} \tag{4.10}$$

and

$$a = \sum_{i=1}^{N} \sum_{j=1}^{N} y_i y_j a_{ij} \quad (a_{ij} \neq \sqrt{a_{ii} a_{jj}}) \tag{4.11}$$

Table 2

Critical Properties and Parameter

Values for CO_2 and CH_2F_2

	CO_2	CH_2F_2	Reference (CO_2,CH_2F_2)
T_c(°R)	547.5	632.8	(12,14)
P_c(psia)	1069.4	845.3	(12,14)
V_c(ft^3/lb.mole)	1.512	1.943	(12,14)
z_c	0.277	0.242	(12,14)
ω	0.225	0.276	-
ω_H	-	0.152	(10)
μ (debye)	0	1.97	(20,20)
Ω_a	0.4470	0.4550	-
Ω_b	0.0911	0.0927	-

where

$$a_{ii} = \frac{\Omega_{ai} R^2 T_{ci}^{2.5}}{P_{ci}} \tag{4.12}$$

$$a_{ij} = \frac{(\Omega_{ai} + \Omega_{aj}) R^2 T_{cij}^{2.5}}{2P_{cij}} \tag{4.13}$$

$$P_{cij} = \frac{z_{cij} R T_{cij}}{v_{cij}} \tag{4.14}$$

$$v_{cij}^{1/3} = 1/2 \ (v_{ci}^{1/3} + v_{cj}^{1/3}) \tag{4.15}$$

$$z_{cij} = 0.291 - 0.08 \left(\frac{\omega_i + \omega_j}{2}\right) \tag{4.16}$$

$$T_{cij} = \sqrt{T_{ci} T_{cj}} \ (1 - k_{ij}) \tag{4.17}$$

The binary constant k_{ij} represents the deviation from the geometric-mean rule for T_{cij}. In general, this constant must be obtained from some experimental information about the binary interaction. Second virial cross coefficients or saturated liquid volumes of binary systems provide good sources of information. For the carbon dioxide - difluoromethane binary, however, such experimental information is not available. Several values of k_{ij} were considered, but these were found to be no improvement over a value of zero. The binary constant was therefore taken to be zero for this system.

When the Redlich-Kwong equation of state and the mixing rules are substituted into Equation (4.5), the fugacity coefficient of component "i" in the mixture becomes

$$\ln \phi_i = \ln \frac{v}{v-b} + \frac{b_i}{v-b} - \frac{2 \sum_{j=1}^{N} y_j a_{ij}}{RT^{3/2} b} \ln \frac{v+b}{b} + \frac{a b_i}{RT^{3/2} b^2} \left[\ln \frac{v+b}{v} - \frac{b}{v+b} \right] - \ln \frac{Pv}{RT} \qquad (4.18)$$

Equation (4.18) was used to calculate the fugacity coefficient at each experimental point. Figures 8, 9, 10, and 11 show these results plotted against the mole fraction carbon dioxide in the vapor phase.

4.4) The Standard-State Fugacities

The activity is completely defined only when the standard-state (or reference-state) fugacity f_i^{0L} is clearly specified. This reference state is quite arbitrary, and its choice is dictated only by convenience. Although it is necessary that f_i^{0L} be the fugacity of component "i" at the same temperature as that of the solution, its pressure and composition may be chosen arbitrarily.

At the temperature levels of this work, both carbon dioxide and difluoromethane are condensable components. That is, the critical temperature of each component is above the temperature of the solution. The standard-state fugacity for each component was then taken to be that pure liquid component at the system temperature. For maximum convenience, a reference pressure of zero was chosen.

The standard-state fugacity is then given by

$$f_i^{0L} = P_i^s \phi_i^s \exp \int_{P_i^s}^{0} \frac{v_i^L}{RT} dP \qquad (4.19)$$

FIGURE 8

Fugacity Coefficients at -60°F

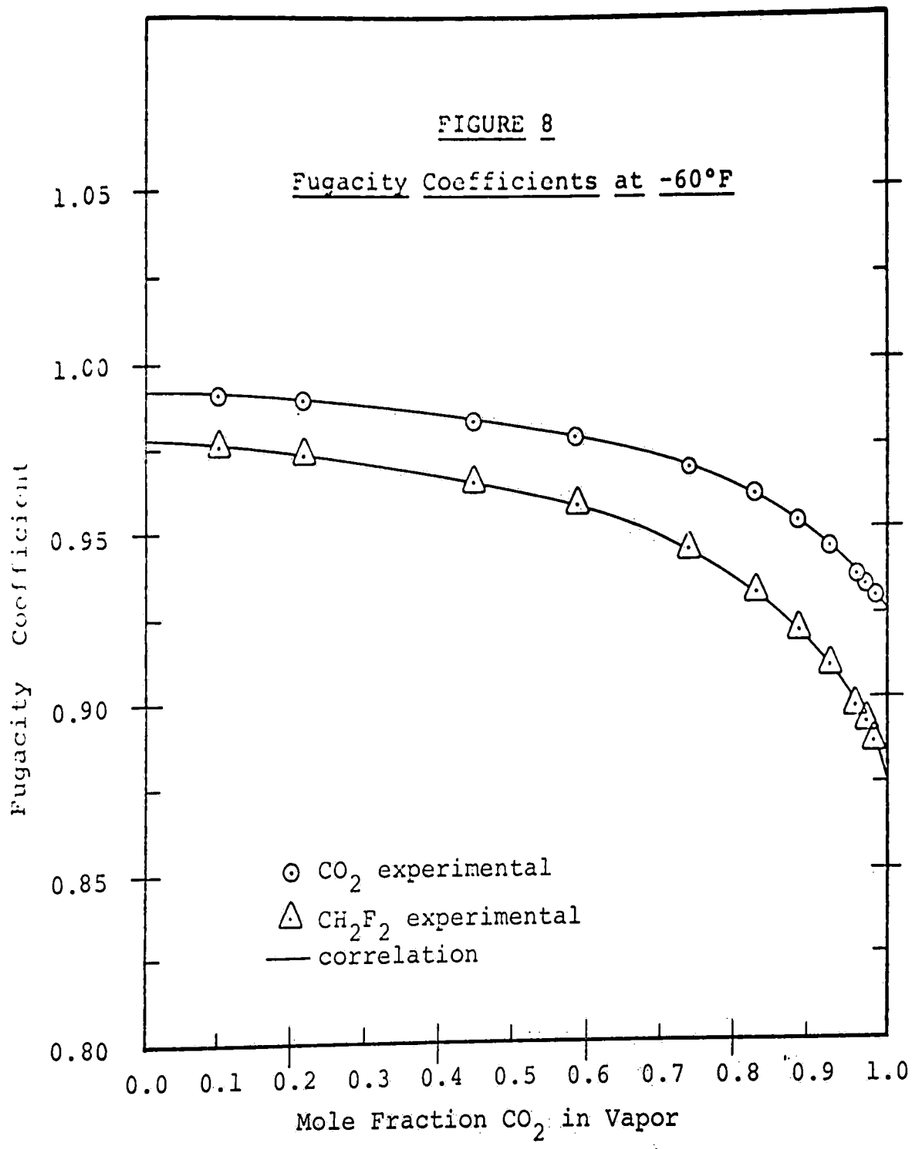

FIGURE 9

Fugacity Coefficients at -20°F

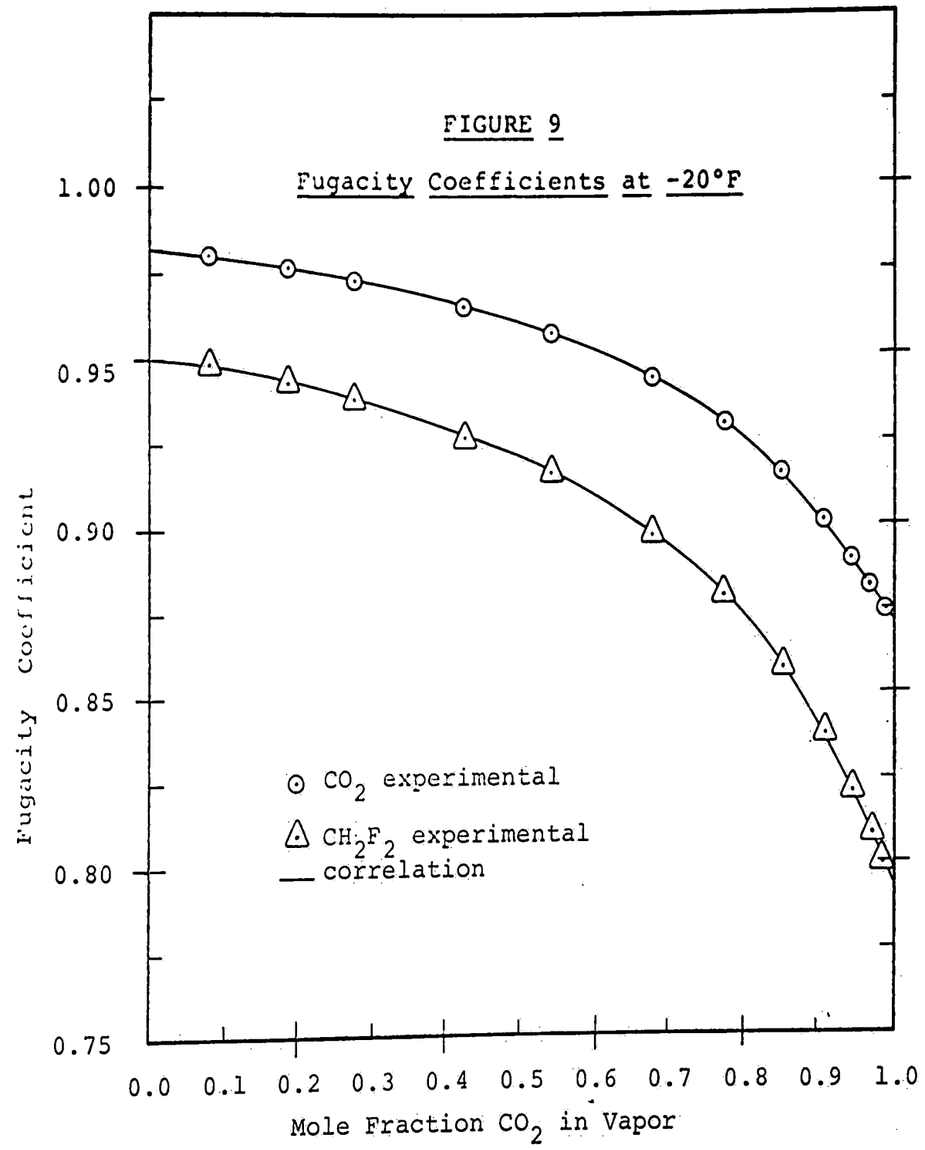

FIGURE 10

Fugacity Coefficients at 20°F

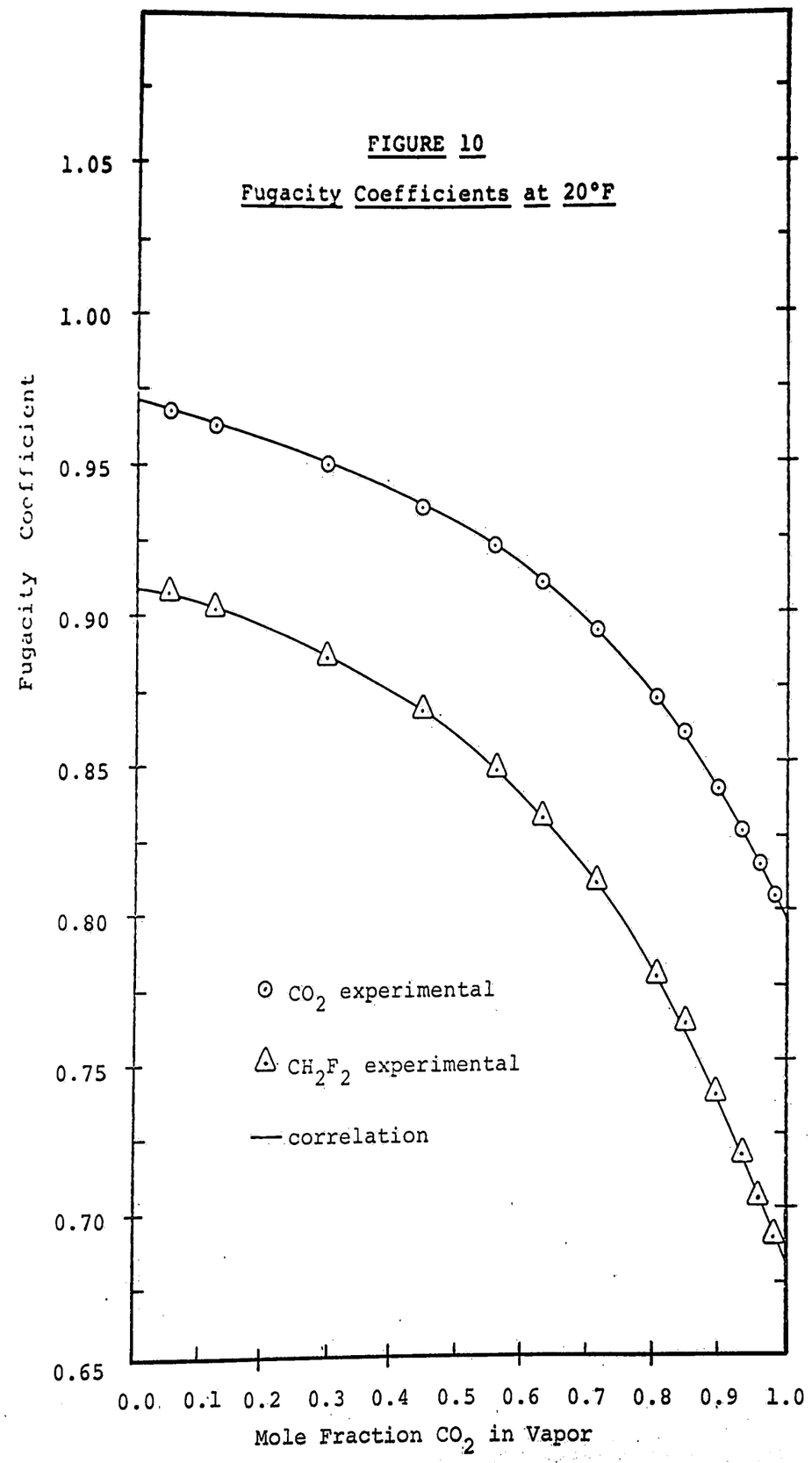

FIGURE 11

Fugacity Coefficients at 50°F

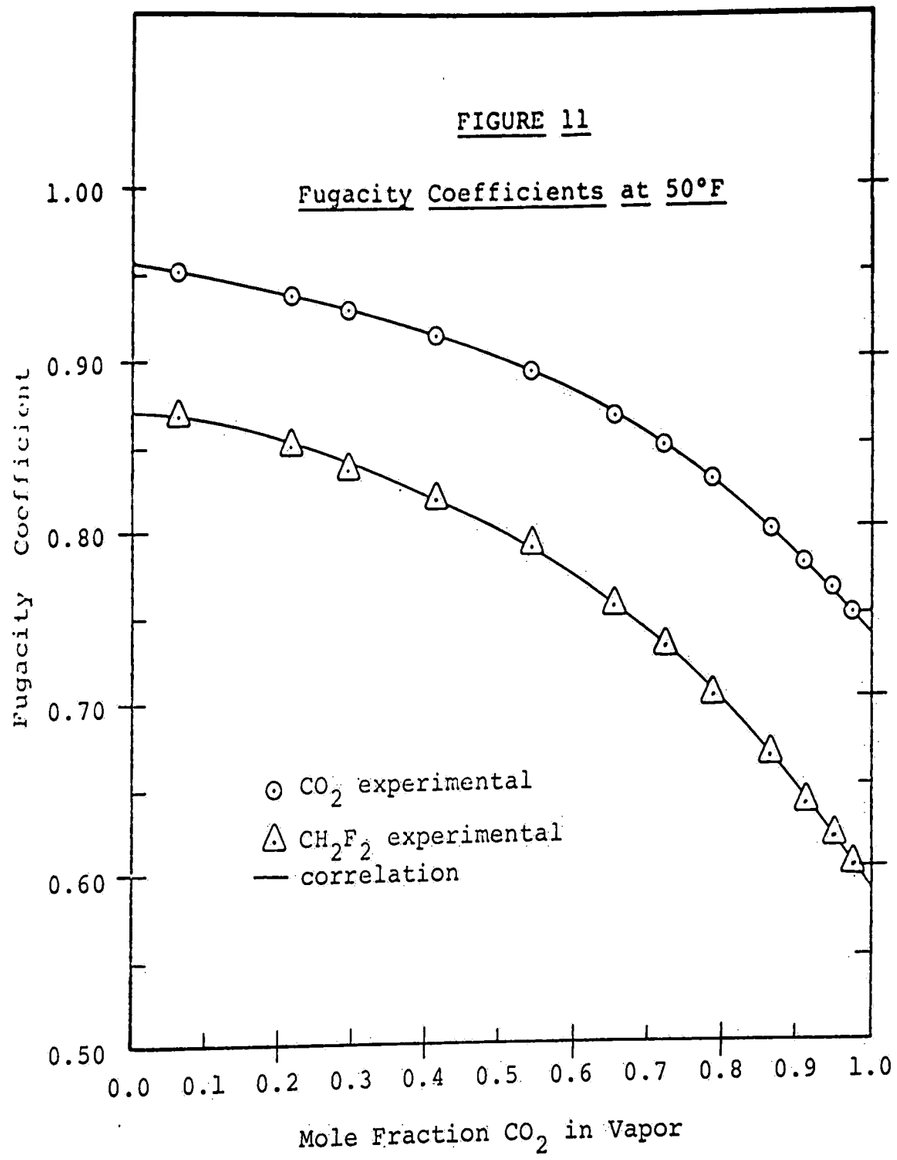

where

P_i^s = saturation (vapor) pressure of pure liquid "i" at temperature T

ϕ_i^s = fugacity coefficient of pure saturated vapor "i" at temperature T and pressure P_i^s

v_i^L = molar liquid volume of pure "i" at temperature T

The vapor pressures were experimentally measured, as described in Section (3.1). The fugacity coefficients of the pure saturated vapors were calculated from the Redlich-Kwong equation of state. The molar liquid volumes for carbon dioxide (13) and difluoromethane (14) at each temperature were obtained from published data.

4.5) The Activity Coefficient

The activity coefficient, at constant temperature, depends on the pressure and the composition. The effects of these two independent variables may be separated by using the exact thermodynamic relation (18)

$$\left(\frac{\partial \ln \gamma_i}{\partial P}\right)_{T,x} = \frac{\bar{v}_i^L}{RT} \qquad (4.20)$$

where $\bar{v}_i^L$ is the partial molar volume of component "i" in the liquid phase.

If an integrated form of the Gibbs-Duhem equation is to be used to correlate isothermal activity-coefficient data, i.e.

$$\sum_i^N x_i \, d \ln \gamma_i = 0 \quad \text{(at constant T,P)} \tag{4.21}$$

it is necessary that these coefficients be evaluated at the same pressure. Experimental activity coefficients obtained at the total pressure of the system, P, can be corrected to a constant, arbitrary reference pressure, P^r, by integration of Equation (4.20):

$$\gamma_i^{(P^r)} = \gamma_i(P) \quad \exp \int_P^{P^r} \frac{\bar{v}_i^L}{RT} \, dP \tag{4.22}$$

The adjusted activity coefficients, $\gamma_i^{(P^r)}$, were normalized such that

$$\gamma_i^{(P^r)} \to 1 \quad \text{as} \quad x_i \to 1 \tag{4.23}$$

The fugacity of each component then becomes equal to the mole fraction times the standard-state fugacity as the composition of the solution approaches that of the pure liquid. In this case, the standard-state fugacity of component "i" is the fugacity of pure liquid "i" at the temperature of the solution and at the reference pressure.

In Section (4.4), a reference pressure of zero was specified. Equation (4.22), when solved for $\gamma_i^{(P)}$, becomes

$$\gamma_i^{(P)} = \gamma_i^{(P0)} \exp \int_0^P \frac{\bar{v}_i^L}{RT} dP \qquad (4.24)$$

Substituting Equations (4.19) and (4.24) into Equation (4.4) gives the result

$$\phi_i y_i P = \gamma_i^{(P0)} x_i P_i^s \phi_i^s \exp\left[\int_{P_i^s}^0 \frac{v_i^L}{RT} dP + \int_0^P \frac{\bar{v}_i^L}{RT} dP\right] \qquad (4.25)$$

For the subcritical components in this study, the partial molar volume $\bar{v}_i^L$ can be equated to the molar liquid volume v_i^L, where v_i^L is assumed to be independent of pressure. Equation (4.25) can then be integrated and solved for $\gamma_i^{(P0)}$ as follows:

$$\gamma_i^{(P0)} = \frac{\phi_i \, y_i \, P}{x_i \, p_i^s \, \phi_i^s \quad \exp\left[\frac{(P - p_i^s) \, v_i^L}{RT}\right]} \tag{4.26}$$

Equation (4.26) was used to calculate all activity coefficients from the experimental data. These results appear in Figures 12, 13, 14, and 15 as the activity coefficient of each component plotted against the mole fraction of carbon dioxide in the liquid phase.

5) CORRELATIVE TECHNIQUE AND RESULTS

5.1) Correlation of Activity Coefficients

The activity coefficients were correlated using an equation developed by Redlich and Kister (19). At conditions of constant temperature and pressure, the excess free energy is related to composition by a series function

$$G^E = RT\, x_1\, x_2\, [B + C\,(x_1 - x_2) + D\,(x_1 - x_2)^2 + \ldots]_{T,P} \qquad (5.1)$$

Differentiation of Equation (5.1) with respect to x_1 gives

$$\ln \frac{\gamma_1}{\gamma_2} = B(x_2 - x_1) + C(6x_1\, x_2 - 1) + D(x_2 - x_1)\,(1 - 8x_1\, x_2) + \ldots \qquad (5.2)$$

Equations can be written for the individual activity coefficients using the relations

$$\ln \gamma_1 = \frac{G^E}{RT} + x_2 \ln \frac{\gamma_1}{\gamma_2} \qquad (5.3)$$

$$\ln \gamma_2 = \frac{G^E}{RT} - x_1 \ln \frac{\gamma_1}{\gamma_2} \qquad (5.4)$$

Substitution of Equations (5.1) and (5.2) into Equations (5.3) and (5.4) gives

$$\ln \gamma_1 = x_1 x_2 [B + C(x_1 - x_2) + D(x_1 - x_2)^2 + \ldots]$$

$$+ x_2 [B (x_2 - x_1) + C(6x_1 x_2 - 1) + D(x_1 - x_2)$$

$$(8x_1 x_2 - 1) + \ldots] \qquad (5.5)$$

$$\ln \gamma_2 = x_1 x_2 [B + C (x_1 - x_2) + D(x_1 - x_2)^2 + \ldots]$$

$$- x_1 [B (x_2 - x_1) + C (6x_1 x_2 - 1) + D (x_1 - x_2)$$

$$(8x_1 x_2 - 1) + \ldots] \qquad (5.6)$$

The experimental data were fit to Equation (5.2) by a second-order least-squares technique. At compositions less than ten mole per cent carbon dioxide, the data exhibited considerable scatter at each temperature level. It will be recalled from Section (2.64) that purification attempts were made to eliminate a distortion of the CO_2 chromatogram by an impurity in the CH_2F_2. Although all observable distortion was successfully eliminated, it is believed that undetectable quantities of the impurity affected the low composition measurements of carbon dioxide. It is in this low composition range also where the totalized count of the electronic integrator is inherently susceptible to the greatest error.

Accordingly, at each temperature level, compositions of less than ten mole per cent CO_2 were discarded in

fitting the data. Figures 12, 13, 14, and 15 show the activity coefficients calculated from the experimental data compared to the fit given by the correlation.

The Redlich-Kister constants at each isotherm were correlated with absolute temperature by a second-order least-squares fit. The results are presented in Table 3.

5.2) Correlation of Fugacity Coefficients

The fugacity coefficients calculated from the Redlich-Kwong equation of state at each isotherm were found to vary linearly with liquid composition. The constants obtained from this fit were in turn found to vary linearly with absolute temperature. These constants are given in Table 4. This correlation greatly facilitated the calculation of pressure-composition diagrams given any temperature and liquid phase composition.

5.3) Prediction of Pressure-Composition Diagrams

The vapor-liquid equilibrium equations for each component as presented in Section (4.1) are

FIGURE 12

Activity Coefficients at -60°F

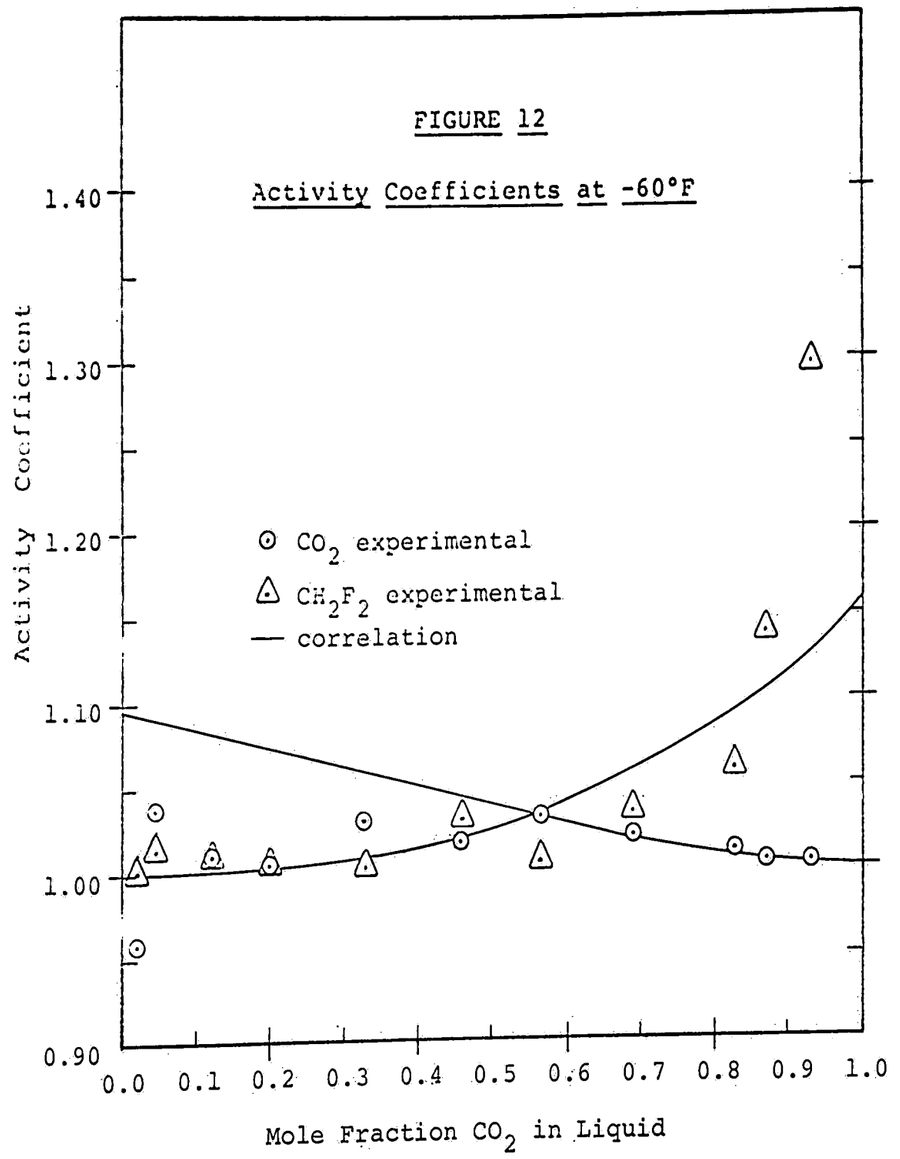

FIGURE 13

Activity Coefficients at -20°F

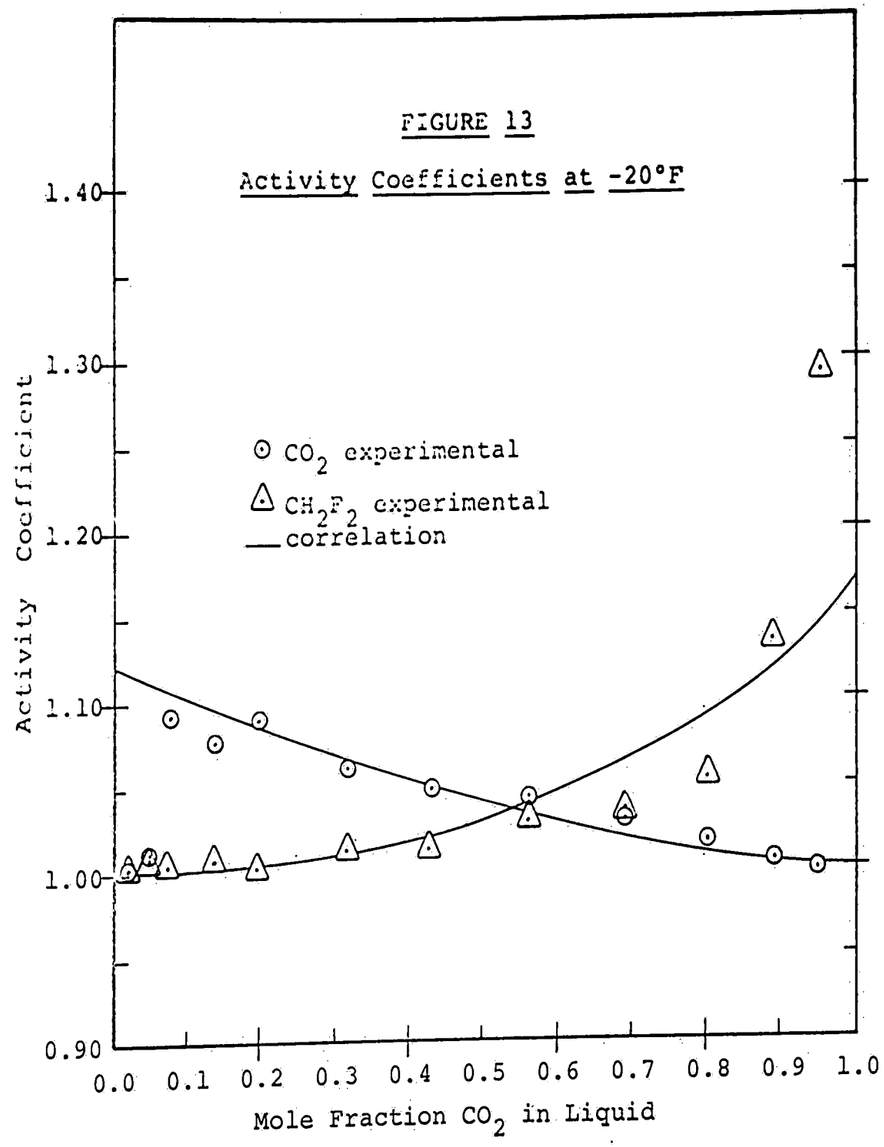

FIGURE 14

Activity Coefficients at 20°F

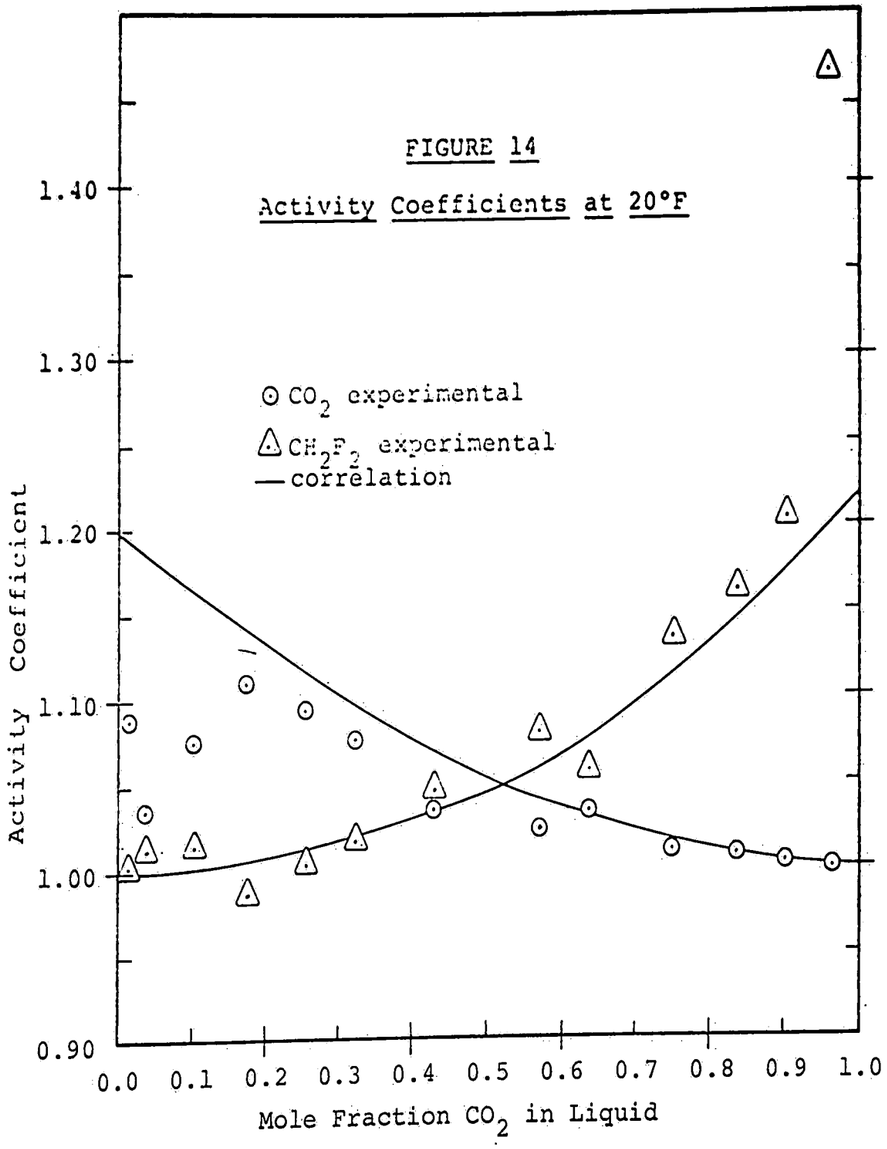

FIGURE 15

Activity Coefficients at 50°F

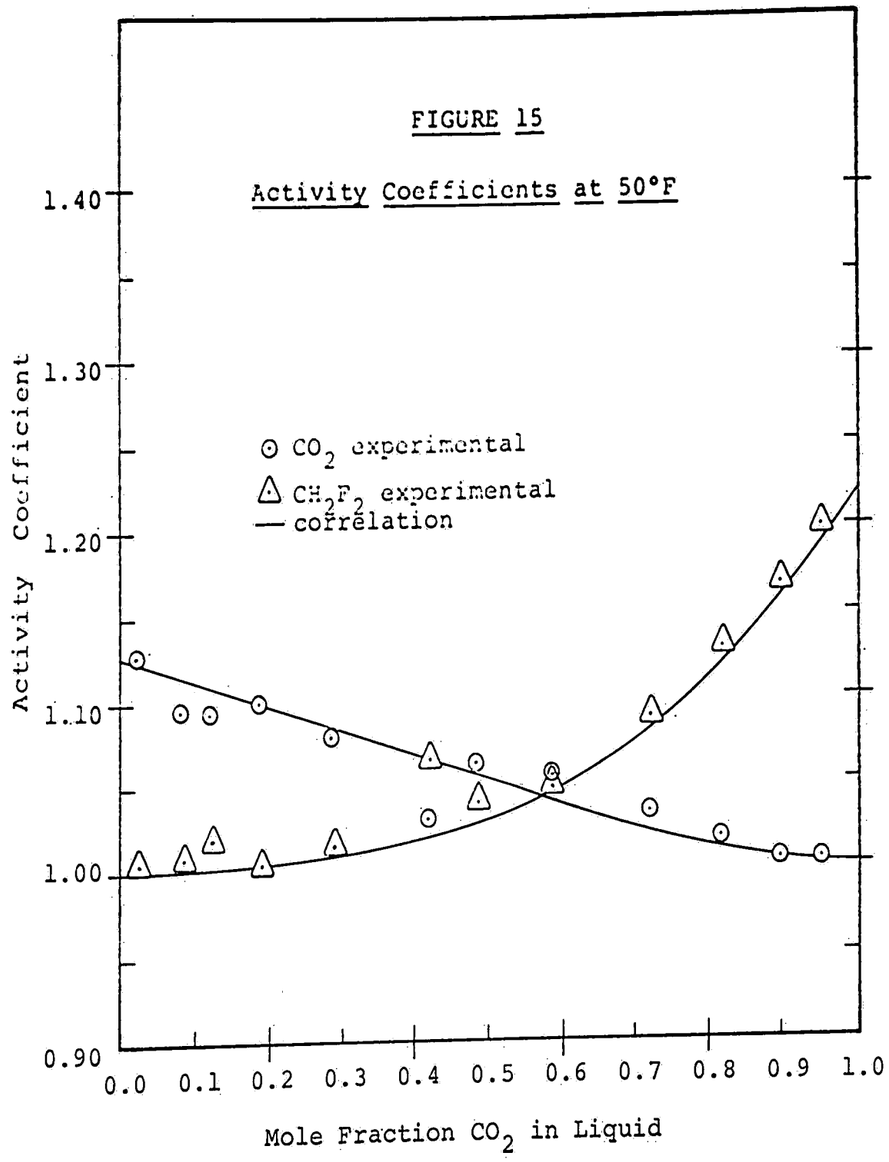

Table 3

Temperature Correlation of Redlich-Kister

Constants (B and C)

$$B = B_0 + B_1 T + B_2 T^2$$

$$B_0 = 4.120003 \times 10^{1},\ B_1 = -2.7760 \times 10^{-1},\ B_2 = 6.200 \times 10^{-4}$$

$$C = C_0 + C_1 T + C_2 T^2$$

$$C_0 = -1.531781 \times 10^{1},\ C_1 = 1.0553 \times 10^{1},\ C_2 = -2.400 \times 10^{-4}$$

T = Absolute Temperature in Deg. Rankine

Table 4

Correlation of Fugacity Coefficients

with Liquid Composition and Temperature

$$\text{PHI } (CO_2) = K + L\,x$$

where x = mole fraction CO_2 in liquid phase

$$K = K_0 + K_1\,T$$

$$K_0 = 1.11943, \quad K_1 = -3.200 \times 10^{-4}$$

$$L = L_0 + L_1\,T$$

$$L_0 = 4.7901 \times 10^{-1}, \quad L_1 = -1.360 \times 10^{-3}$$

$$\text{PHI } (CH_2F_2) = M + N\,x$$

$$M = M_0 + M_1\,T$$

$$M_0 = 1.36346, \quad M_1 = -9.600 \times 10^{-4}$$

$$N = N_0 + N_1\,T$$

$$N_0 = 5.8614 \times 10^{-1}, \quad N_1 = -1.700 \times 10^{-3}$$

T = Absolute Temperature in Deg. Rankine

$$\phi_1 y_1 P = \gamma_1 x_1 P_1^s \phi_1^s \exp\left[\frac{v_1^L}{RT}(P - P_1^s)\right] \qquad (5.7)$$

$$\phi_2 y_2 P = \gamma_2 x_2 P_2^s \phi_2^s \exp\left[\frac{v_2^L}{RT}(P - P_2^s)\right] \qquad (5.8)$$

As a first approximation of pressure, the exponential terms may be taken as unity, and Equations (5.7) and (5.8) may be combined as follows:

$$P = \frac{\gamma_1 x_1 P_1^s \phi_1^s}{\phi_1} + \frac{\gamma_2 x_2 P_2^s \phi_2^s}{\phi_2} \qquad (5.9)$$

Using the correlations developed in this section, Equation (5.9) may be solved for pressure given any temperature and liquid-phase composition. Equations (5.7) and (5.8) can then be solved for the respective vapor-phase compositions. Pressure-composition diagrams were calculated at each temperature using this procedure. The results are shown in Figures 4, 5, 6, and 7.

5.4) Predictive Consequences of an Ideal Liquid Phase

As discussed in Section (3.2), the liquid phase behaved nearly ideally at all temperature levels. This ideality increased with decreasing temperature. The liquidus curves at -60 and -20°F were nearly linear. It can be shown that the straight liquidus curve allows prediction of the vapor phase curve from only the pure component vapor pressures. The expression for this prediction, derived in Appendix C, has the following form:

$$P = \frac{1}{y_1 \, (1/P_1^s - 1/P_2^s) + 1/P_2^s} \qquad (5.10)$$

where CO_2 is denoted as component 1 and CH_2F_2 as component 2.

Equation (5.10) was used to predict the pressure-composition diagrams at -60 and -20°F. A comparison of this prediction with the experimental data is presented in Figures 16 and 17. Maximum deviations in predicted pressure of five and two per cent at -60 and -20°F,

FIGURE 16

Pressure-Composition Diagram at -60°F from Ideal Liquid Phase Correlation

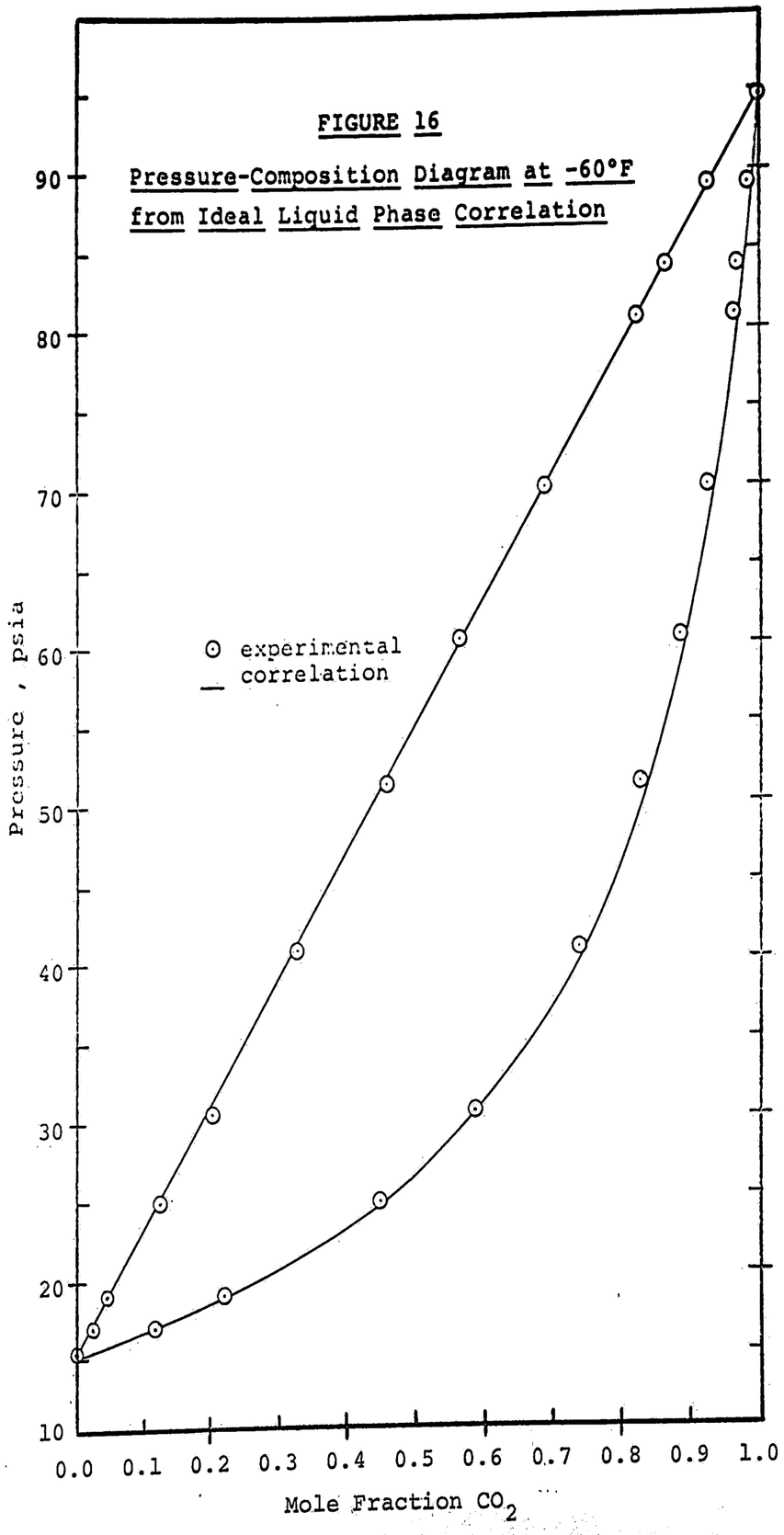

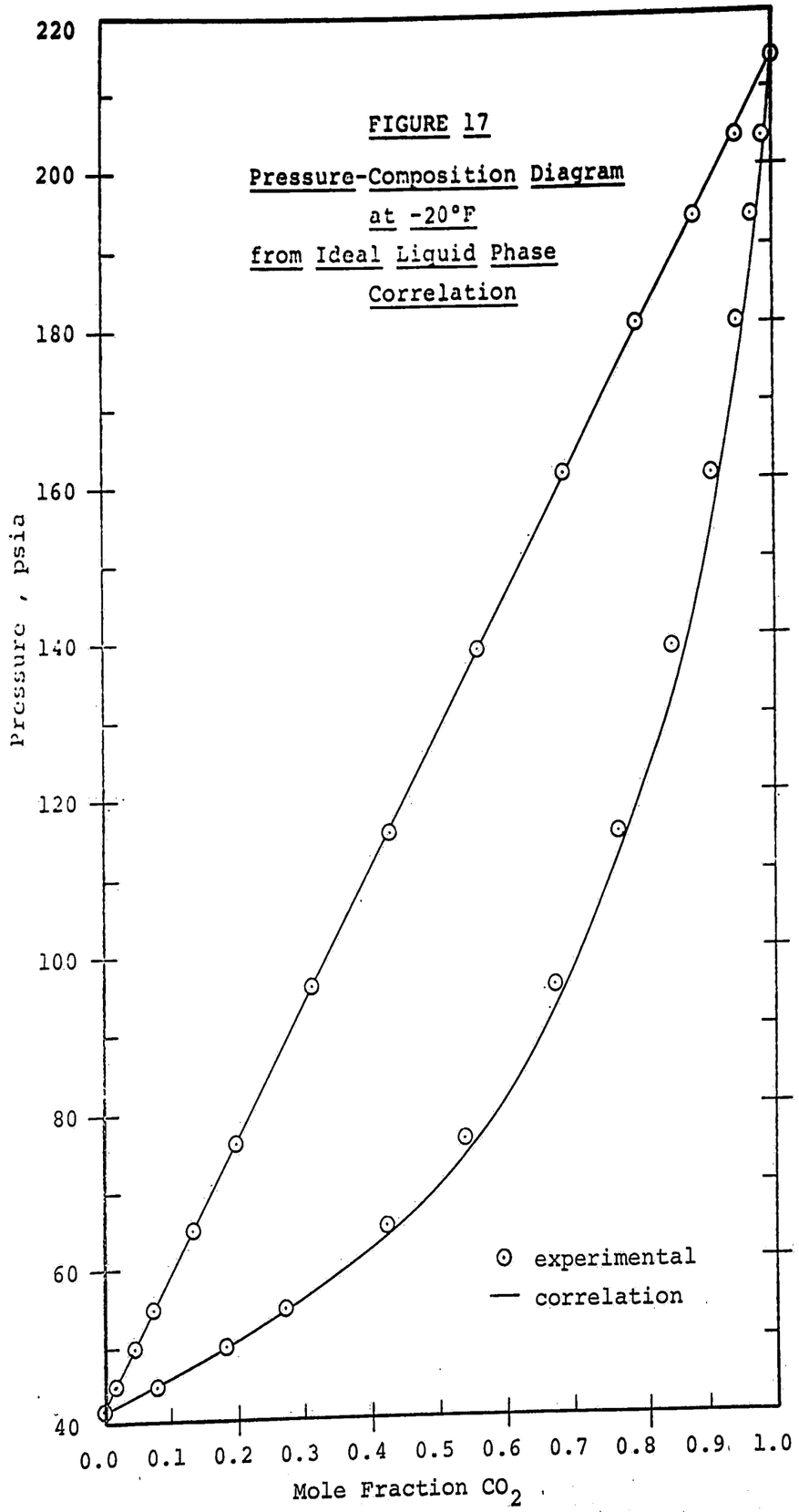

FIGURE 17

Pressure-Composition Diagram at -20°F from Ideal Liquid Phase Correlation

respectively, were observed. These deviations may be accounted for by the fact that the liquidus curves, although nearly straight, were not perfectly linear. In both cases, however, the shapes of the predicted vapor curves were nearly identical to those constructed by fitting a smooth curve through the experimental data points. At 20 and 50°F, the liquidus curves exhibited some curvature and this technique was found not to be valid.

6) APPENDICES

APPENDIX A

Calibration Data

Table A-1

Compositions of the Primary Standards

Primary Standard Number	Ideal Gas Composition Mole Per Cent		Real Gas Composition Mole Per Cent	
	CO_2	CH_2F_2	CO_2	CH_2F_2
4	1.07	98.93	1.04	98.96
51	5.08	94.92	4.98	95.02
7	10.06	89.94	9.87	90.13
71	24.83	75.17	24.54	75.46
5	49.95	50.05	49.77	50.23
6	74.76	25.24	74.79	25.21
1	90.04	9.96	90.11	9.89
2	94.88	5.12	94.92	5.08
3	98.87	1.13	98.88	1.12

Table A-2

Compositions of the Secondary Standards

Secondary Standard Number	Composition Mole Per Cent	
	CO_2	CH_2F_2
8	1.81	98.19
14	4.12	95.88
4	8.43	91.57
2	22.17	77.83
7	47.60	52.40
6	74.87	25.13
5	90.52	9.48
3	95.08	4.92
1	98.75	1.25

APPENDIX B

Experimental Data

Table B-1

Experimental Data at -60°F

Pressure, psia	Liquid Mole Fraction, CO_2	Vapor Mole Fraction, CO_2
15.18	0.000	0.000
16.60	0.0200	0.101
18.80	0.0440	0.213
24.67	0.124	0.447
30.20	0.199	0.587
40.60	0.324	0.737
51.10	0.458	0.825
60.30	0.564	0.882
70.00	0.688	0.924
80.80	0.822	0.961
83.90	0.864	0.969
89.10	0.927	0.982
94.60	1.000	1.000

Table B-2

Experimental Data at -20°F

Pressure, psia	Liquid Mole Fraction, CO_2	Vapor Mole Fraction, CO_2
41.6	0.000	0.000
44.7	0.0190	0.0790
49.5	0.0480	0.183
54.4	0.0730	0.275
64.9	0.135	0.424
75.9	0.197	0.540
95.6	0.313	0.676
115.1	0.429	0.771
138.8	0.560	0.847
161.1	0.689	0.904
180.4	0.798	0.942
193.8	0.883	0.965
204.0	0.944	0.982
214.2	1.000	1.000

Table B-3

Experimental Data at 20°F

Pressure, psia	Liquid Mole Fraction, CO_2	Vapor Mole Fraction, CO_2
95.2	0.000	0.000
99.7	0.0140	0.0510
107.1	0.0370	0.120
127.7	0.103	0.296
149.4	0.173	0.442
175.2	0.252	0.556
197.0	0.320	0.628
227.7	0.427	0.712
273.4	0.567	0.804
297.7	0.633	0.847
333.9	0.747	0.895
363.5	0.831	0.932
386.5	0.898	0.959
408.5	0.960	0.981
422.4	1.000	1.000

Table B-4

Experimental Data at 50°F

Pressure, psia	Liquid Mole Fraction, CO_2	Vapor Mole Fraction, CO_2
161.0	0.000	0.000
171.0	0.0200	0.0620
198.0	0.0810	0.215
217.1	0.120	0.294
244.6	0.186	0.414
290.3	0.286	0.543
348.5	0.418	0.656
387.6	0.483	0.721
438.4	0.583	0.789
503.9	0.719	0.863
553.0	0.814	0.910
592.2	0.893	0.948
624.4	0.949	0.975
651.6	1.000	1.000

APPENDIX C

DERIVATIONS

Derivation of the Equation Predicting the Pressure-Composition Diagram for a Binary Mixture Whose Liquid Phase Behaves Ideally

Denoting carbon dioxide as component 1 and difluoromethane as component 2, the vapor-liquid equilibrium equations for each component are

$$\phi_1 y_1 P = \gamma_1 x_1 f_1^{0L} \qquad (C\text{-}1)$$

$$\phi_2 y_2 P = \gamma_2 x_2 f_2^{0L} \qquad (C\text{-}2)$$

Equations (C-1) and (C-2) may be solved for x_1 and x_2, respectively, and added, to give

$$1 = P\left(\frac{\phi_1 y_1}{\gamma_1 f_1^{0L}} + \frac{\phi_2 y_2}{\gamma_2 f_2^{0L}}\right) \qquad (C\text{-}3)$$

Noting that $y_2 = (1 - y_1)$, Equation (C-3) can be written

$$1 = P\left[y_1 \left(\frac{\phi_1}{\gamma_1 f_1^{0L}} - \frac{\phi_2}{\gamma_2 f_2^{0L}} \right) + \frac{\phi_2}{\gamma_2 f_2^{0L}} \right] \tag{C-4}$$

Solving for pressure gives

$$P = \frac{1}{y_1 \left(\frac{\phi_1}{\gamma_1 f_1^{0L}} - \frac{\phi_2}{\gamma_2 f_2^{0L}} \right) + \frac{\phi_2}{\gamma_2 f_2^{0L}}} \tag{C-5}$$

Equations (C-1) and (C-2) may be similarly manipulated to eliminate y_1 and y_2. The resulting equation is

$$P = x_1 \left(\frac{\gamma_1 f_1^{0L}}{\phi_1} - \frac{\gamma_2 f_2^{0L}}{\phi_2} \right) + \frac{\gamma_2 f_2^{0L}}{\phi_2} \tag{C-6}$$

Equation (C-6) is the equation of a straight line of slope ($\gamma_1 f_1^{0L} / \phi_1 - \gamma_2 f_2^{0L} / \phi_2$) and intercept ($\gamma_2 f_2^{0L} / \phi_2$), expressing the relationship between the CO_2 liquid mole fraction, x_1, and the total system pressure, P.

When the system is composed of pure difluoromethane, the system pressure is the vapor pressure of CH_2F_2 at the system temperature. Setting $x_1 = 0$ in Equation (C-6) reveals that the vapor pressure of CH_2F_2 is given by ($\gamma_2 f_2^{0L} / \phi_2$). Similarly, when the system is composed of pure carbon dioxide, $x_1 = 1$ in Equation (C-6), and the vapor pressure of CO_2 at the system temperature is given by ($\gamma_1 f_1^{0L} / \phi_1$).

Equation (C-5) may therefore be rewritten as

$$P = \frac{1}{y_1 \left(\frac{1}{p_1^s} - \frac{1}{p_2^s} \right) + \frac{1}{p_2^s}} \qquad \text{(C-7)}$$

Thus, for a binary mixture whose liquid phase behaves ideally, Equation (C-7) predicts the vapor phase curve from only the pure component vapor pressures.

7) NOMENCLATURE

a,b	-	constants in Redlich-Kwong equation of state
B, C, D	-	Redlich-Kister constants
B	-	second virial coefficient
f	-	fugacity, psia
f^{0L}	-	standard-state fugacity for the pure liquid at the temperature of the solution, psia
G^E	-	excess free energy, Btu/lb.mole
k_{ij}	-	binary interaction constant
p	-	pressure, psia
R	-	gas constant, 10.73 psia · ft^3/lb.mole · °R
T	-	temperature, °R, unless otherwise noted
T_R	-	reduced temperature
V	-	total volume of vapor mixture
v	-	molar volume of vapor phase, ft^3/lb.mole
$\bar{v}$	-	partial molar volume in the liquid phase, ft^3/lb.mole
x	-	liquid-phase mole fraction
y	-	vapor-phase mole fraction
z	-	compressibility factor

Greek Letters

γ	-	liquid-phase activity coefficient
η	-	association constant
μ	-	dipole moment, debye
ϕ	-	vapor-phase fugacity coefficient
Ω_a, Ω_b	-	dimensionless constants in Redlich-Kwong equation of state
ω	-	acentric factor
ω_H	-	acentric factor of the homomorph of the polar component

Superscripts

L	-	liquid phase
p	-	calculated at total pressure of system
p^r	-	calculated at reference pressure r
p0	-	calculated at zero pressure
r	-	reference pressure
s	-	saturation
V	-	vapor phase

Subscripts

c	-	critical point
i	-	component "i"
j	-	component "j"
ii	-	pure component "i"
jj	-	pure component "j"
ij	-	interaction between components "i" and "j"
1	-	carbon dioxide
2	-	difluoromethane

8) REFERENCES

1. Weber, H. C., and Meissner, H. P. "Thermodynamics for Chemical Engineers." John Wiley & Sons, Inc., New York, 1963.

2. Smith, J. M., and Van Ness, H. C. "Introduction to Chemical Engineering Thermodynamics." McGraw-Hill Book Company, Inc., New York, 1959.

3. Zeeninger, H. "Determination of Vapor-Liquid Equilibria at Elevated Pressure by Calorimetric Analysis." Chem. Ing. Tech., 26, p. 327, 1954.

4. Thorp, N., and Scott, R. L. "Fluorocarbon Solutions at Low Temperatures I." J. Phys. Chem., 60, p. 1441, 1956.

5. Croll, I. M., and Scott, R. L. "Fluorocarbon Solutions at Low Temperatures IV." J. Phys. Chem., 68, p. 3853, 1964.

6. Piacentini, A. "An Experimental and Correlative Study of the Vapor-Liquid Equilibria of the Tetrafluoromethane-Trifluoromethane System." Ph.D. Dissertation, Lehigh University, 1966.

7. Stein, F. P., Sterner, C. J., and Geist, J. M. "Vapor-Liquid Equilibrium Apparatus for Cryogenic Systems." Chem. Eng. Prog., 58, p. 70, 1962.

8. Smolcha, R. P. "An Experimental Investigation of the Co-Existing Liquid and Vapor Phases of Solutions of Tetrafluoromethane and Chlorotrifluoromethane." M.S. Thesis, Lehigh University, 1968.

9. Pitzer, K. I., and Curl, R. F., Jr. "Volumetric and Thermodynamic Properties of Fluids." J. Am. Chem. Soc., 79, p. 2369, 1957.

10. Prausnitz, J. M., et al. "Computer Calculations for Multicomponent Vapor-Liquid Equilibria." Prentice-Hall, Inc., Englewood Cliffs, 1967.

11. Martin, J. J., and Hou, Y. C. "Development of an Equation of State for Gases." A.I.Ch.E. J., 1, p. 142, 1955.

12. Martin, J. J., Kapoor, R. M., and DeNevers, N. "An Improved Equation of State for Gases." A.I.Ch.E. J., 5, p. 159, 1959.

13. American Society of Refrigerating Engineers. "Refrigerating Data Book." New York, 1952.

14. Malbrunot, P., et al. "Pressure-Volume-Temperature Behavior of Difluoromethane." J. Chem. Eng. Data, 13, p. 16, 1968.

15. Beattie, J. A. Chem. Rev., 44, p. 141, 1949.

16. Redlich, O., and Kwong, J.N.S. Chem. Rev., 44, p. 233, 1949.

17. Cheuh, P. L., and Prausnitz, J. M. "Vapor-Liquid Equilibria at High Pressures. Vapor Phase Fugacity Coefficients in Nonpolar and Quantum Gas Mixtures." Ind. Eng. Chem. Fund., 6, p. 492, 1967.

18. Cheuh, P. L., and Prausnitz, J. M. "Vapor-Liquid Equilibria at High Pressures: Calculation of Partial Molar Volumes in Nonpolar Mixtures." A.I.Ch.E. J., 13, p. 1099, 1967.

19. Redlich, O., and Kister, A. T. "Algebraic Representation of Thermodynamic Properties and the Classification of Solutions." Ind. Eng. Chem., 40, p. 345, 1948.

20. National Bureau of Standards. "Selected Values of Electric Dipole Moments for Molecules in the Gas Phase." NSRDS-NBS 10, Washington, D.C., 1967.

21. Keyes, F. G., and Kinney, A. W. "Thermodynamic Properties of Carbon Dioxide." Am. Soc. Refr. Eng. J., pp. 17-43, 1917.

22. Hála, E., et al. "Vapour-Liquid Equilibrium." Pergamon Press, New York, 1958.

23. Hougen, O. A., Watson, K. M., and Ragatz, R. A. "Chemical Process Principles." Part II, John Wiley & Sons, Inc., New York, 1959.

24. Lewis, G. N., and Randall, M. Revised by Pitzer, K. S., and Brewer, L. "Thermodynamics." McGraw-Hill Book Company, New York, 1961.

25. Technical Bulletin B-2. "Freon." E. I. Du Pont de Nemours and Company, Wilmington, 1964.

9) VITA

The author was born on December 7, 1945, in New York, New York, the son of Walter and Helen Adams. He was graduated, with honors, from the Bronx High School of Science, in 1962.

Mr. Adams received the Bachelor of Science degree in Chemical Engineering and the Bachelor of Arts degree in Chemistry from Bucknell University in 1967. At Bucknell, he served as President of Alpha Chi Sigma Professional Honorary Fraternity, Secretary of the American Institute of Chemical Engineers, and a member of the American Chemical Society. He then began his graduate studies at Lehigh University as a National Defense Education Act Fellow, and was awarded the Master of Science degree in Chemical Engineering in 1969.

The author has been employed for summers by the Gulf Oil Corporation, Philadelphia, Pennsylvania, as a Process Engineering Trainee, and by the Procter and Gamble Manufacturing Company, Staten Island, New York, as a Production Management Trainee. He is currently engaged as a Process Engineer with the M. W. Kellogg Company in New York City.